Comparison between two numerical modelling approaches for delta morphodynamics applied on the Roda Sandstone Formation

Xueyao Chen

TU Delft

Comparison between two numerical modelling approaches for delta morphodynamics applied on the Roda Sandstone Formation

by

Xueyao Chen

to obtain the degree of Master of Science
at the Delft University of Technology,
to be defended publicly on Wednesday December 3, 2025 at 09:00 AM.

Student number:	5903432	
Project duration:	January, 2025 – November, 2025	
Thesis committee:	Dr. S. C. Toby,	TU Delft, supervisor
	Dr. G. Rongier,	TU Delft, supervisor
	Dr. A. Baar,	TU Delft, committee member

TU Delft

Abstract

Deltas play an important role in the energy transition for their potential in subsurface applications like geothermal applications and Carbon Capture and Storage. During delta formation, the interplay between coupled forcings governs the internal architecture of the delta, leading to heterogeneity in the subsurface, which is critical for subsurface applications, as it affects fluid flow, heat transport and storage capacity and makes modelling essential for understanding the internal structure of the delta. This study uses the Roda Sandstone (the Roda X) as a case study, chosen for its well-preserved stratigraphy and documented lobe-sublobe hierarchy. This research evaluates whether DeltaRCM, a Reduced-Complexity Model, can produce a delta model of stratigraphy that is comparable to the Roda X, with an emphasis on the internal lobes. The research compares the modelling results from DeltaRCM with those from the existing Delft3D model and field data, using both surface and subsurface metrics. Under the parameter settings in this research, DeltaRCM generates delta models with strong channel incisions rather than distributary, lobe-like geometries, which do not resemble the lobe–sublobe hierarchy documented in the Roda X. The findings suggest that DeltaRCM requires further refinement or parameter adjustment to reproduce realistic lobe structures before it is used for subsurface applications.

Preface

I have never imagined that one day I could really graduate from TU Delft. Now I am making it.

I would like to show great gratitude to my supervisors, Stephan Toby and Guillaume Rongier. Both have been so helpful to me and encouraged me to move forward in my difficult times. My supervisors have also shown great passion and precision in Earth Sciences, which set examples for working in the industry. I would also like to thank Anne Baar for her comments on improving my thesis and presentation.

For the research, I would also express my gratitude to Equinor and Deltares, who have provided the Delft3D model for me to use. I have always wanted to use Delft3D for modelling since OUC time, and this wish came true with their help.

I would like to thank my family who have supported me for years. I cannot express my gratitude with words. I would have never made it this far without them.

Additionally, I would like to thank you to Arin for the support and help in the last two years.

My life has never been easy in the last two years, as it always takes longer for me to achieve anything. So many people have shown kindness to me during this period, and also helped me develop myself in terms of personal growth. I would say thank you to you all.

As my study is approaching the end, I have more time for reflection. I increasingly feel that I am so blessed for all the opportunities and support I have ever received over the years to have my own growth and the opportunity to broaden my horizon. After so many things going on in my life and the world, the will to explore and learn still does not perish. In the end, I hope graduation from TU Delft is the end of my studies and also the start of my next period of life.

Xueyao Chen
The Hague, November 2025

Contents

List of Figures

List of Tables

1 Introduction

1.1. Importance of delta modelling

Deltas play a crucial role in the energy transition towards a sustainable society (Bhattacharya, 2006; Bauer et al., 2013), as they provide reservoirs for Carbon Capture and Storage (CCS) and geothermal projects (Wright, 1985; Ojo and Tse, 2016). Research worldwide has examined deltaic reservoirs to assess their potential for energy applications. For example, in the Niger Delta, the potential to transform depleted deltaic gas fields into CCS reservoirs is promising (Ojo and Tse, 2016). Research has also shown that the Deltaic Frio Formation in the Texas Gulf Coast has technical and economic value for geothermal power (Ortiz-Sanguino et al., 2022).

Understanding the internal architecture and heterogeneity of deltaic reservoirs is essential for predicting flow behaviour and storage performance. The internal structure of deltas is governed by the complicated interplay of hydraulic and morphological forcings, which shape different sedimentary units in the deltaic environment, like facies distribution and sandbody geometries (Geleynse et al., 2011). The spatial distribution of heterogeneities at various scales, including the layout of sedimentary facies and the characteristics of river channels and sand bodies, can directly affect the characteristics and behaviour of deltaic reservoirs and flow paths in subsurface applications (Graham et al., 2015).

To understand the characteristics and geometry of deltaic reservoirs, numerical modelling is commonly used to construct models for delta evolution and stratigraphic architecture. The traditional approach to numerical modelling uses geostatistics based on geological data, which requires prior knowledge of the existing structure (Michael et al., 2010). In contrast, forward process-based modelling simulates delta formation by solving the governing equations and allows models with realistic geometries that are not limited by assumptions about spatial structure (Michael et al., 2010). Among them, Delft 3D is currently one of the most integrated physics-based formation models (Lesser et al., 2004; Liang et al., 2015). However, computational fluid dynamics (CFD)-based methods like Delft3D are computationally demanding.

Reduced-complexity models (RCMs) like DeltaRCM require less computation and allow greater flexibility in changing the timesteps of spatial and temporal parameters (Bokulich, 2013; Liang et al., 2015; Chan et al., 2023). DeltaRCM uses a weighted random walk algorithm to simulate flow and sediment and has been successfully applied and modified to produce models that resemble the topography of multiple deltas (e.g., Liang et al., 2015; Lauzon et al., 2019; Chan et al., 2023). However, most existing applications focus on modelling delta surface morphology, and relatively limited research has examined its ability to reproduce subsurface stratigraphic architecture (Xu et al., 2021). Furthermore, limited research has compared the DeltaRCM model with field data or Delft3D in terms of stratigraphic realisation (Liang et al., 2015).

This study aims to address this research gap by using DeltaRCM to construct a geological model of the Eocene deltaic Roda Sandstone in the Spanish Pyrenees (Joseph et al., 1993). Roda Sandsone has

well-exposed outcrops that show the stratigraphic architecture of a fluvial delta at different hierarchical levels by the stacking of small-scale deltaic sublobes in larger lobe complexes (A. W. Martinius, 2017), together with the cementation of abandoned lobe surfaces, which compartmentalises the sandstone in a reservoir context and can influence flow in subsurface systems. These characteristics, together with the abundant field data and well-constrained stratigraphy, make it an ideal case for model validation. Previous studies and an existing Delft3D model provide a valuable reference for understanding the geological feature and cross-comparison.

The primary objective of this study is to assess whether DeltaRCM can produce a delta model of stratigraphy comparable to the Roda Sandstone, with a particular focus on investigating whether internal lobe structures can be generated using a simpler algorithm. The comparison between DeltaRCM outputs, Delft3D results and field data aims to assess the efficiency and accuracy of DeltaRCM in generating a realistic stratigraphic model. The outcome provides insight into the applications of reduced-complexity models for geological reservoir modelling and their potential in energy transition research.

1.2. Research Questions

In the research, the main research question is defined:

Can we use a simpler and faster approach than Delft3D to generate a stratigraphic model similar to the Roda X?
To address this question comprehensively, the following sub-questions are defined:

- **What are the key input parameters needed for building the DeltaRCM model?**
  To generate the DeltaRCM model, a series of input parameters related to the formation of the delta must be specified and entered into a table. These hydrodynamic and morphodynamic parameters need to be collected from the literature and simulations. Additionally, it is essential to test the robustness and sensitivity of the model using various input values.
- **Can DeltaRCM generate the lobe-like geometries at different scales, like those observed in the Roda Sandstone?**
  Through this research, RCM is used to build a model that has similarities to what is observed in the field.
- **What are the key similarities and differences between the stratigraphic architecture modelled by DeltaRCM and Delft3D, and the architecture deduced from field measurements?**
  The DeltaRCM model needs to be compared with existing field data and Delft3D models. To check its performance, physical parameters about the geometry and reservoir characteristics of the generated delta model will need to be compared.

2

Case Study: The Roda Sandstone

The Roda Sandstone is the target formation for modelling in this research. An introduction to the Roda Sandstone will cover its geological setting and characteristics, particularly the architecture and hierarchy within the Roda X unit, to provide a basic understanding of the modelling background for the following chapters.

2.1. Location and tectonic settings

The Roda Sandstone is located in the Tremp–Graus Basin, which lies within the south-central part of the South Pyrenean Foreland Basin in the Huesca Province, Spain (Joseph et al., 1993; Leren et al., 2010). The South Pyrenean foreland basin is a WNW to ESE-oriented, elongated feature opening and deepening to the west towards the Atlantic Ocean (Tinterri et al., 2007). Differential movements within the basin led to its fragmentation and, consequently, to the formation of the piggyback Tremp-Graus Basin (Leren et al., 2010).

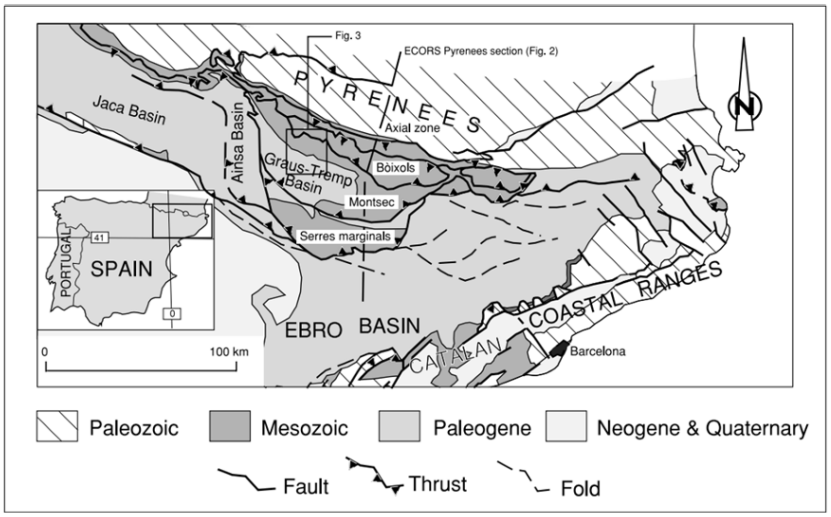

Figure 2.1: Geology map of the Roda adapted from López-Blanco et al., 2003

During the Eocene, the geometry and configuration of the Tremp-Graus basin were influenced by thrust displacement associated with the Pyrenean orogeny, specifically the Boixols and Montsec thrusts as in Figure 2.1 (Tinterri et al., 2007; Leren et al., 2010; Olariu et al., 2012). The latter generated the syncline that acted as the deposition centre for the 'piggyback' basin and accommodated shallow marine deposition, including the Roda Sandstone and other marine sedimentation. (Puigdefàbregas et al., 1992; Tinterri et al., 2007; Leren et al., 2010). The Roda Sandstone was deposited syntectonically in the NE

margin of the basin, close to the active thrust front (Eichenseer and Luterbacher, 1992; Leren et al., 2010).

2.2. Characteristics of the Roda Sandstone

The Roda Sandstone consists of shallow-marine, siliciclastic-carbonate mixed deposits up to 200 m thick and is biostratigraphically dated to around 50 Ma in late Ypresian (Leren et al., 2010). Shallow-marine carbonate units bound it, namely the Avelina Limestone and the Morillo Limestone Formation (Leren et al., 2010). Additionally, the Plateau Limestone is deposited between members of the Roda Formation, which represents stable conditions of the basin, as shown in the Figure 2.2.

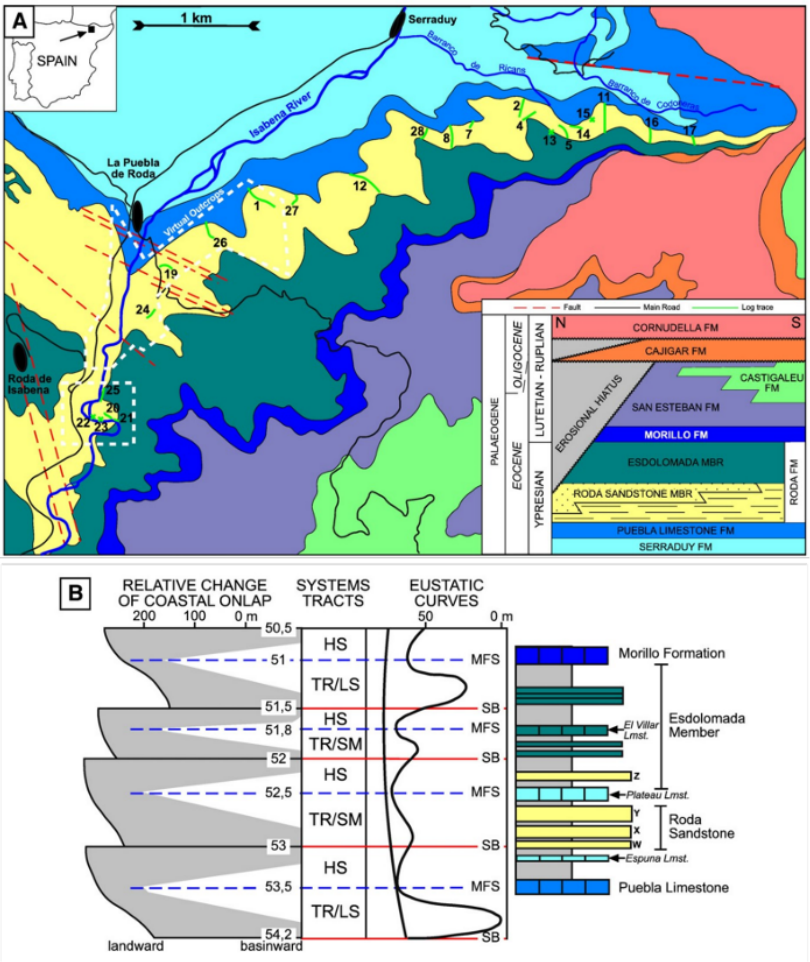

Figure 2.2: (A) Geological map of the northern Isabena Valley showing measured log sections (Leren et al., 2010) and the lithostratigraphic column, modified from Molenaar and Martinius, 1990. (B) Stratigraphic section ranging from the Puebla to the Morillo formations exhibiting sequences and system tracts. Abbreviations: MFS: maximum flooding surface, SB: sequence boundary, SM: shelf-margin, HS: highstand, TR: transgressive, and LS: lowstand (Leren et al., 2010). Adapted from Alghamdi, 2023

The Roda Sandstone mainly consists of 6 deltaic sandstone bodies, namely U, V, W, X, Y, Z, and shows a trend of coarsening and shallowing upwards (Joseph et al., 1993). These sandstone bodies were deposited in a Gilbert-type delta system, each representing a prograding sand lobe. The sand lobes display a seaward progradational pattern from Northeast to Southwest (Figure 2.4), and each sand lobe is formed by smaller-scale delta sublobes that stack vertically and laterally (A. W. Martinius, 2017). The sublobes are formed by wave-induced flow and deposited contemporaneously with elongated tidal sandstone bodies (A. W. Martinius, 2017). These sandstone bodies, both lobes and sublobes, are capped by fossilous carbonate cemented horizons as shown in Figure 2.4 (Leren et al., 2010; Coll

et al., 2013; A. W. Martinius, 2017). The development of these carbonate cementations in the Roda Formation occurred in distinct stages and affected the lithification of these layers (A. Martinius and Molenaar, 1991).

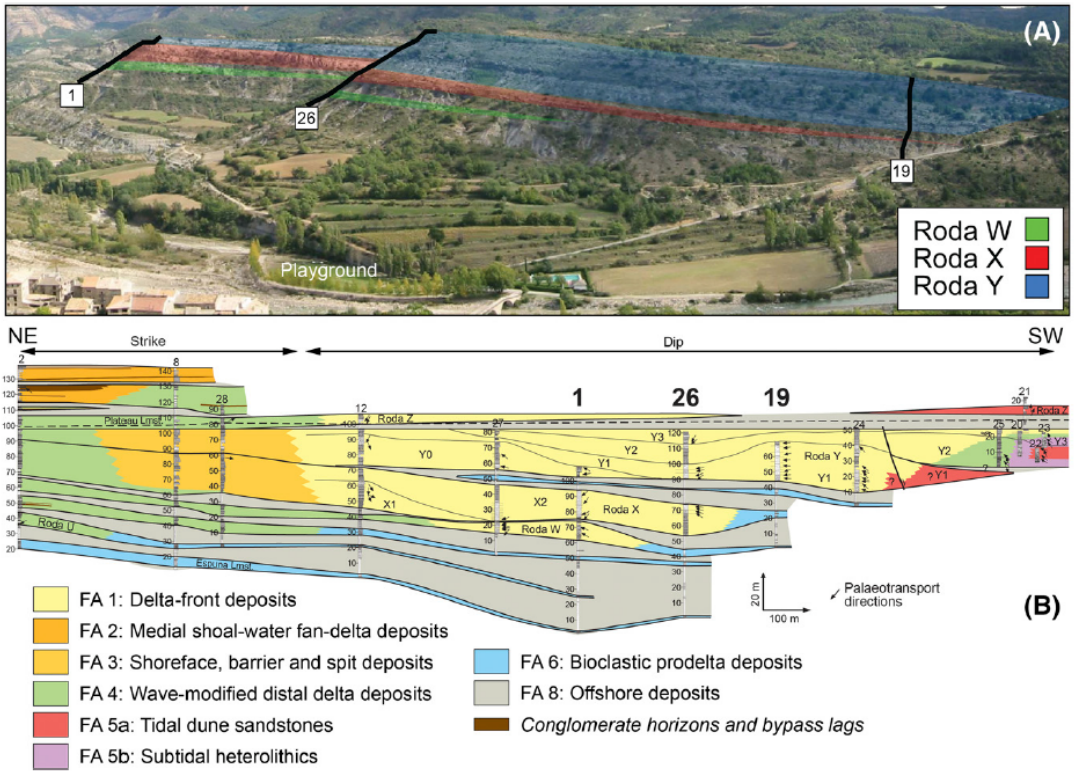

Figure 2.3: (A) Panoramic view of the Roda Sandstone W, X, Y along the Isabena valley. (B) Log correlation panel from the Roda Sandstone outcrops along the eastern side of the Isabena Valley (Leren et al., 2010; A. W. Martinius, 2017).

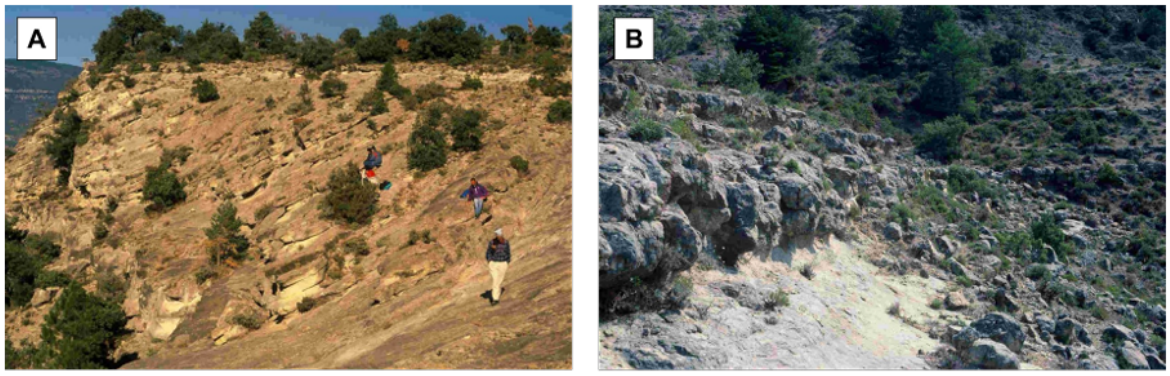

Figure 2.4: (A) An outcrop photograph showing sets of clinoforms of a sand lobe composed of medium to coarse sands (Crumeyrolle, 2003). (B) Carbonate-cemented bed capping one of the prograding sand lobes (Crumeyrolle, 2003). Adapted from Alghamdi, 2023.

The Roda Sandstone is dominantly arkosic with sediments derived from the granitic axial zone in the Pyrenees (Muñoz, 1992), which are predominantly sand with a relatively low clay fraction, and the finer sediments are mostly silt (Chanvry, 2016). These sediments entered the Tremp-Graus basin in an NNE-SSW paleochannel (Puigdefabregas et al., 1985, Leren et al., 2010). Lobes in the Roda Sandstone responded quickly to variations in sediment supply and accommodation space by undergoing autocyclic lobe switching and abandoning channels during delta formation, leading to large unconfor-

mities at lobe boundaries (Leren et al., 2010, A. W. Martinius, 2017). The absence of channel incisions in the outcrop also supports the interpretation that deposition was dominated by the progradation of lobes. Wave and tidal reworking of lobe tops occurred in the formation process and changed the geometry of lobes in all the sandstone bodies (Leren et al., 2010, A. W. Martinius, 2017).

Among all the sandstone bodies in the Roda Sandstone, the Roda X is chosen to be the target formation to study whether DeltaRCM can be used to generate models that resemble the lobes. This unit has been the focus of several previous numerical models and is supported by field observations and quantitative measurements for validation (Joseph et al., 1993; Leren et al., 2010; A. W. Martinius, 2017; Deltares, 2024). The Roda X exhibits an overall progradational pattern from NE to SW with partial aggradation. The sedimentary units can be divided into five sublobes X3 – X7 based on modelling field observation as indicated in Figure 2.5 (Joseph et al., 1993; A. W. Martinius, 2017).

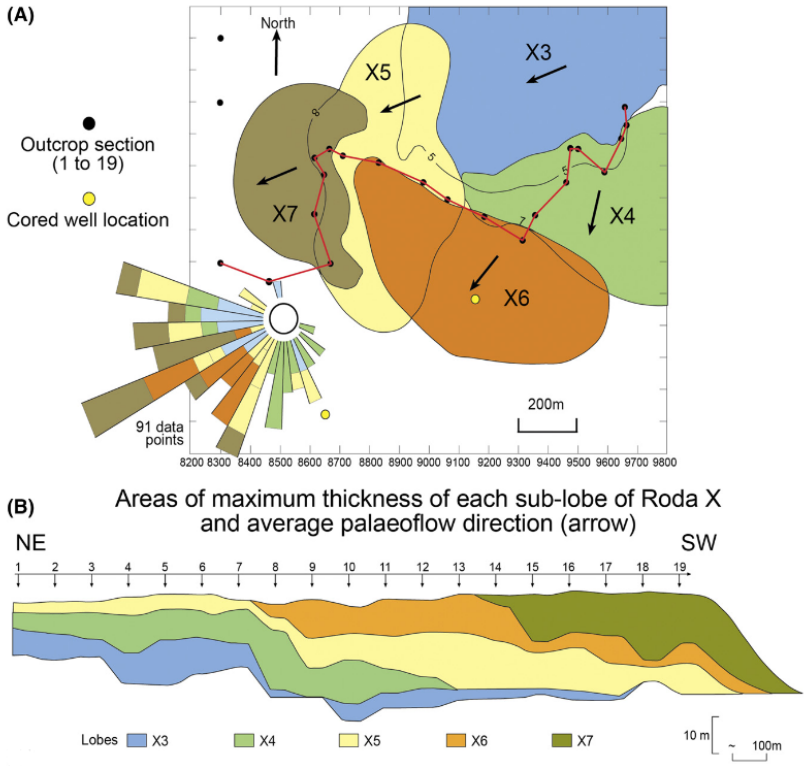

Figure 2.5: (A) Schematic map representation of five Roda X sublobes based on field data. (B) Cross-section along a northeast to southwest line of Roda X based on field data. (Adapted from Leren et al., 2010 and A. W. Martinius, 2017).

Different facies are observed and recorded in the field log for the Roda X along Isabena Valley. The facies change from wave-modified delta at the proximal part to medial shoreface, barrier, and spit deposits, and massive delta-front deposits at the distal end. As the Roda X formation pinches into the subsurface, bioclastic prodelta deposits are witnessed in Figure 2.3.

The Roda X has a length of 1.3km and a width of 1.5 km, with a thickness of 5–20m in the NE-SW direction, as indicated by field data. The dimensions of the sublobes in the Roda X are recorded in detail in the table below by measurements from map view and cross-section view in Table 2.1.

Sublobes	Length (km)	Width (km)	NE–SW cross-section maximum length (km)	Thickness (m)
X3	0.9	0.6	1.2	10
X4	0.7	0.5	1.2	10
X5	1.1	0.5	1.6	15
X6	1.0	0.5	1.4	12
X7	0.6	0.3	0.8	20
Total	1.5	1.3	2.1	5–20

Table 2.1: Dimensions of the Roda X based on Leren et al., 2010 and A. W. Martinius, 2017.

The total volume of the Roda X is calculated as $26.8 \times 10^8 m^3$ from the schematic representation of field data from Leren et al., 2010. Meanwhile, a previous geostatistics model based on log and well data estimated the volume to be around $32.3 \times 10^8 m^3$ (Joseph et al., 1993), which is consistent with the magnitude of the result from direct calculation (see Table 2.2).

Sublobes	Calculated volume ($\times 10^8 m^3$)	Modelled volume ($\times 10^8 m^3$)
X3	5.4	5.9
X4	3.5	4.7
X5	8.3	8.2
X6	6.0	10.4
X7	3.6	3.3
Total	26.8	32.3

Table 2.2: Calculated volume using field data from Leren et al., 2010 and A. W. Martinius, 2017 and Modelled volume from Joseph et al., 1993.

The difference likely arises because the estimate from direct calculation is based on top-view measurements from the geological map rather than accurate subsurface geometry. Map-view orientation can diverge from the direction of maximum thickness in the outcrop. Thus, the estimate may not include all the geobodies in the subsurface. These field data, modelling results and sources of uncertainties will provide another dimension for model comparison in the following chapters.

3

Methodology

This chapter presents the methodology to evaluate if DeltaRCM can generate a geological model that is similar to the observed features of the Roda X and how its performance compares with the existing Delft3D model. This chapter first introduces the modelling framework of Delft3D and DeltaRCM, then it describes the setup of the DeltaRCM model and sensitivity tests in detail. Eventually, to quantify model outputs, a few surface and subsurface metrics are presented.

3.1. Modelling methods

A reference model for Delft3D is provided for this research by Equinor and Deltares (Deltares, 2024). Accordingly, this section summarises the Delft3D framework before introducing the detailed DeltaRCM set-up.

3.1.1. Delft3D

A reference numerical model is provided by Deltares for this research using the Delft3D modelling suite (version 4) that couples the flow module (Delft3D-FLOW) and the wave module (Delft3D-WAVE) (Deltares, 2024). The flow module (Delft3D-FLOW) solves the non-linear shallow water equations of incompressible, turbulent flow based on the Navier-Stokes equations (Lesser et al., 2004). It simulates sediment transport, along with the associated morphology and stratigraphy in the reference model and is coupled with the wave model to incorporate wave-induced changes to the modelled hydrodynamics and morphodynamics using the SWAN (Simulating WAVES Nearshore) model (Deltares, 2024). To accelerate the morphological evolution in the simulated process, a morphological scale factor (morfac) is applied to multiply the computed bed elevation changes at each hydrological timestep (Deltares, 2024).

3.1.2. DeltaRCM

DeltaRCM is a reduced-complexity model that utilises a weighted random walk algorithm, which includes hydrodynamic and morphodynamic components to simulate flow and sediment processes in the domain (Liang et al., 2015). Unlike Delft3D, which explicitly solves the shallow-water equations, DeltaRCM calculates water and sediment movement using probabilistic rules derived from physical principles, namely inertia, gravity, and flow resistance (Liang et al., 2015; Lauzon et al., 2019).

At each timestep, the inlet water discharge through the channel is divided into water parcels and routed within the domain using a weighted random walk (Liang et al., 2015; Lauzon et al., 2019). The probability field determines the direction along which each parcel moves, with higher probabilities assigned to paths of greater water depth and lower local slope resistance. The resulting water parcel paths establish local water flow and then dictate the dispersal of sediment parcels in the routing scheme. Sediment parcels are represented by sand and mud, where sand is routed as bedload and mud is fully suspended load (Liang et al., 2015; Moodie et al., 2021). Erosion and deposition occur based on local transport capacity and flow velocity following the Meyer–Peter and Müller (Meyer-Peter and Müller,

1948) relation,

$$q_{s,\mathrm{cap}} = q_{s0}\left(\frac{u_{\mathrm{loc}}}{u_0}\right)^{\beta}, \tag{3.1}$$

where u_{loc} is the depth-averaged flow velocity in the cell, β is an exponent (default $\beta = 3$), q_{s0} is the unit–width upstream sand flux at the inlet, and u_0 is a reference velocity. At each step, sand is either deposited on or eroded from the bed depending on u_{loc} and the local sand flux $q_{s,\mathrm{loc}}$ (i.e., the flux entering from upstream):

$$\text{Deposit if} \quad q_{s,\mathrm{loc}} > q_{s,\mathrm{cap}}, \tag{3.2}$$

$$\text{Erode if} \quad u_{\mathrm{loc}} > u_{\mathrm{ero}}^{\mathrm{sand}} \ \text{ and } \ q_{s,\mathrm{loc}} < q_{s,\mathrm{cap}}, \tag{3.3}$$

Where $u_{\mathrm{ero}}^{\mathrm{sand}}$ is the sand erosion threshold velocity ($coeff_{u_{\mathrm{ero}}^{\mathrm{sand}}}$).

Mud, as a fully suspended washload, does not have a local capacity; It is deposited or eroded solely based on u_{loc} relative to threshold velocities at each timestep.

$$\text{Deposit if} \quad u_{\mathrm{loc}} < u_{\mathrm{dep}}^{\mathrm{mud}}, \tag{3.4}$$

$$\text{Erode if} \quad u_{\mathrm{loc}} > u_{\mathrm{ero}}^{\mathrm{mud}}, \tag{3.5}$$

with $u_{\mathrm{dep}}^{\mathrm{mud}}$ and $u_{\mathrm{ero}}^{\mathrm{mud}}$ given by parameters $coeff_{u_{\mathrm{dep}}^{\mathrm{mud}}}$ and$coeff_{u_{\mathrm{ero}}^{\mathrm{mud}}}$, respectively.
During sediment routing, the volumes of passing sediment parcels and preserved bed sediment are exchanged at each parcel timestep, dictating deposition and erosion at the grid. Bed elevation is then updated based on mass conservation from lateral and cross-slope topographic sediment dispersal (Liang et al., 2015; Lauzon et al., 2019). The routing paths are then updated accordingly.

This research utilises pyDeltaRCM, developed by Moodie et al., 2021, which provides a Python interface for the existing DeltaRCM model and its subsequent stratigraphic analysis.

3.2. DeltaRCM model set-up

The DeltaRCM model inherits several settings from the Delft3D model by Deltares (2024), including bathymetric data and the magnitudes of forcings, which allows direct inter-model comparisons. Some parameters are adjusted in the research to ensure model stability.

3.2.1. Bathymetric data

The computational domain of the DeltaRCM model spans 14,100 m in the horizontal (x) direction and 10,250 m in the vertical (y) direction, with a uniform spatial resolution of 50 m × 50 m. The initial model bathymetry is based on a 500 m-wide and 1 km-long river, with an inlet channel width of 500m, flowing into a trapezoidal-shaped marine basin with a width of 14,100 m and a length of 9,750m. At the river mouth of the inlet channel, the water depth is 4 meters below sea level and increases to around 18 meters below sea level at the seaward model boundary, corresponding to a bed slope of 0.1°. To prevent overbank flow across the landward boundary, the riverbank area is set at 5 meters above sea level. Figure 3.1 shows the bathymetry and shoreline (Deltares, 2024).

3.2.2. Forcings and sediment supply

The domain is forced by a constant river discharge of 1,100 m³/s at the inlet, which provides the source of water and sediment supply for the system. The value corresponds to the upper-bound discharge from the Delft3D model, because tests with a constant lower discharge (< 750 m³/s) and a linearly decreasing discharge (1,100 m³/s - 250 m³/s) led to numerical instability and terminated the runs. Thus, the constant 1,100 m³/s water discharge is used to ensure model stability. Waves, tides and wind are not included in the DeltaRCM model function. Water and sediment parcels will be routed cell to cell within the domain, and parcels exiting the offshore boundary will be removed. In contrast, lateral and upstream land boundaries are closed for routing.

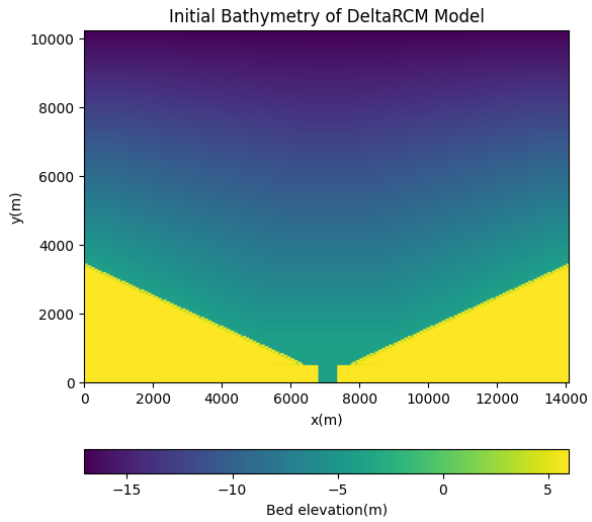

Figure 3.1: Bathymetry of DeltaRCM model

The inlet sediment feed controls sediment availability in DeltaRCM, which provides the primary source of delta deposits. The bed in the DeltaRCM model consists of only sand. At the inlet, a 90% sand and 10% mud proportion is used (Deltares, 2024, which is higher than the average 24% bedload proportion of modern rivers (Cohen et al., 2022). However, the sand fraction used for the DeltaRCM model is consistent with field observations from Roda X, as mud is barely seen in the outcrop. A sediment concentration of C_0 = 0.1% of the water discharge volume is used. With a constant discharge of 1100m³/s, the implied total volumetric sediment flux is 1.1m³/s, with sand being 0.99m³/s and mud being 0.11m³/s.

Additionally, subsidence is applied to the seafloor as a spatially varying vertical change to the seabed, allowing for accommodation space in the Delft3D model (Deltares, 2024). It increases linearly from 0m per timestep to 0.012m per timestep in the seaward direction(y), generating a cumulative subsidence of 0m at the river mouth and 12m at the seaward boundary by the end of the simulation.

To build a model with a comparable volume to the Delft3D model, a total timestep of 1000 is chosen for all DeltaRCM models, corresponding to 1052.19 days in the base model during the simulated process, which takes approximately 5 hours.

3.2.3. Parameters

The table below shows the detailed parameters used for the base DeltaRCM model, along with their sources and explanations.

Name	Value	Unit	Explanation
Length (L)	10250	m	Trimmed from the vertical dimension (y) by Deltares, 2024
Width (W)	14100	m	Trimmed from the horizontal dimension (x) by Deltares, 2024
Resolution (dx)	50	m	The same resolution as the Delft3D model for further comparison
Land thickness ($L0\_meters$)	500	m	The same length of inlet channel from the Delft3D model by Deltares, 2024
Velocity (u_0)	0.55	m/s	Calculated from Deltares, 2024 for constant discharge 1100m^3/s
Channel width (N_0_meters)	500	m	The same as the channel width from Deltares, 2024
Inlet water depth ($h0$)	4	m	The same inlet depth from Deltares, 2024
Sediment concentration (C_0)	0.1	%	Commonly used in DeltaRCM research (Liang et al., 2015; Hariharan et al., 2021)
Number of sediment parcels (Np_sed)	5000	#	A sufficient number of sediment parcels will result in a more regular sediment deposition and smoother bed elevation (Moodie and Passalacqua, 2021)
Number of water parcels (Np_water)	5000	#	A sufficient number of water parcels will result in a smoother water surface(Moodie and Passalacqua, 2021)
Bedload sand fraction ($f\_bedload$)	0.9	#	The fraction of sand in total sediment supply and bedload composition from Deltares, 2024
Sand erosion velocity threshold ($coeff_{u_{\mathrm{ero}}^{\mathrm{sand}}}$)	1.05	m/s	Default setting for morphology by Liang et al., 2015
Mud erosion velocity threshold ($coeff_{u_{\mathrm{ero}}^{\mathrm{mud}}}$)	1.5	m/s	Default setting for morphology by Liang et al., 2015
Sand deposition velocity threshold ($coeff_{u_{\mathrm{dep}}^{\mathrm{sand}}}$)	0.3	m/s	Default setting for morphology by Liang et al., 2015

Table 3.1: Parameters and values used in the DeltaRCM base model

These parameters provide a controlled baseline for comparison with the Delft3D model. Using consistent geometry and sediment flux allows direct assessment of how the process influences the resulting delta morphology and stratigraphy.

3.3. Sensitivity test

To evaluate the robustness of the DeltaRCM model and deepen understanding of how parameters influence deltaic development, three sensitivity tests are conducted with different parameter settings, focusing on sediment concentration and river discharge. All the models maintain the same total sediment input volume as the Delft3D model to ensure comparability, which is achieved by

$$V_s = Q_s * T = Q * c_0 * T = \ constant \tag{3.6}$$

where v_s is the total sediment volume, Q_s is the sediment flux, Q_s is the water discharge, c_0 is the inlet sediment concentration, and T is the simulation time.

The inlet velocity is determined by:

$$u_0 = \frac{Q}{N_0 * h_0} \tag{3.7}$$

where N_0 = 500m represents the inlet width and and h_0 = 4m is the inlet depth.

Table 3.2 summarises the parameters for each scenario. Apart from the parameters explicitly listed, all the other parameters are identical to the base case, as in Table 3.1. The corresponding results are presented and analysed in the following chapter with the Delft3D model and field data.

Model name	Inlet Velocity (m/s)	Discharge (m^3/s)	Sediment concentration (%)	Simulated time (days)
Base model	0.55	1100	0.1	1,052.19
Double Discharge model	1.10	2200	0.1	526.09
Low Concentration model	0.55	1100	0.05	2104.36

Table 3.2: Parameters for the sensitivity test

3.4. Model output quantification

To systematically compare the Delft3D and DeltaRCM models, several surface and subsurface metrics were defined to quantify the morphological and stratigraphical evolution of the delta. Except for sand thickness, net-to-gross ratio (NTG), and virtual logs, which are computed at the end of the run, all the metrics are calculated at unified non-dimensional times, expressed as fractions of the total timesteps. This allows comparison between models at equivalent stages of delta evolution, independent of physical time scales (Deltares, 2024). To better identify morphological changes at the channel scale, all metrics are computed and visualised within a cropped domain measuring 5,500 m in length (y) and 8,000 m in width (x).

3.4.1. Surface metrics

Elevation (Unit: m)
Elevation is the calculated bed elevation relative to sea level. In DeltaRCM and Delft3D, the metric is a direct output of the model. Comparing elevations between models provides an overview of the large-scale topographic evolution and the development of depositional patterns.

Delta area (Unit: m^2)
Delta area is defined as the planform area where net deposition occurred above the reference sea level. It is calculated as the number of cells with elevations above sea level multiplied by the grid cell area. This approach follows the definition used by Liang et al. (2015), and represents the areal footprint of the deltaic deposit formed during the simulation.

Delta length (Unit: m)
Delta length measures the seaward advance of the shoreline along the centreline in dip direction, following the same principle as delta area measurement. It is defined as the distance from the inlet to the last cell above sea level to ensure consistency with the observed elevation output. The measurement can provide information about how the delta front progrades in the modelled time.

Active deposition cells (#)
The active deposition cells count indicates the morphological growth of the delta. It is calculated by counting the cells that elevate at least 0.001m at the timestep. This metric indicates the spatial extent of active sedimentation. Tracking active pixels over time reveals whether the model exhibits focused channel activity or widespread reactivation, while monitoring the distribution of active deposition cells indicates where the delta progradation occurs. High values indicate periods of active lobe growth and distributary expansion, and lower values indicate channel merging or abandonment.

3.4.2. Subsurface metrics

Volume (Unit: m^3)
Volume calculates the cumulative sediment deposition relative to the initial seabed. The computed volume of the DeltaRCM model is cross-checked against the theoretical sediment input at the river mouth to ensure consistency. It is computed as the sum of the elevation change between the final and initial topographies, with the final topography corrected for subsidence.

Sand thickness (Unit:m)
The sand thickness calculates the cumulative thickness of sand preserved in the stratigraphy. Similar to Sandplover (“sandplover”, 2021), which is the official visualisation package for DeltaRCM models. The calculation tracks the last time a sand parcel visited each grid. At each timestep, the deposited sand thickness is added to the local preserved column, and erosion removes sediment proportionally according to the sand fraction of the existing layer.

Net-to-gross (NTG) (#)
NTG records the proportion of sand within the total preserved stratigraphy at the end of the simulation. It is calculated as the ratio of preserved sand to the total stratigraphic thickness in each grid cell and computed simultaneously with the preserved sand thickness. This metric provides an estimate of reservoir quality and offers a direct view of sand distribution.

3.4.3. Logs
To enable intermodel comparison and direct comparison with field data, four virtual sand fraction logs are created individually at the distal, medial, proximal, and one location slightly off the inlet channel in the chosen DeltaRCM model based on Deltares (2024). The preserved sand fraction log employs a similar boxy stratigraphy method, inspired by sandplover (“sandplover”, 2021), where each timestep contributes erosion or deposition to the vertical stack of the grid, resulting in a layer-by-layer evolution of the stratigraphy without interpolation. The resulting logs capture the temporal evolution of the local facies through the model run and provide insight into the depositional environment.

Together, these metrics from surface and subsurface provide the basis for assessing the performance of DeltaRCM model with comparison to Delft3D and field data.

4

Results

In this chapter, the results of the DeltaRCM models are presented and further compared with those of the Delft3D model and the Roda field data. Both Delft3D and DeltaRCM models generate deltaic morphologies, but they differ in the pattern of morphology and preserved stratigraphy due to different modelling methods. The first part focuses on surface metrics that reveal sediment transport and distribution during delta evolution. The second part with subsurface metrics illustrates how these surface features are recorded stratigraphy through modelled aggradation, progradation and erosion. Aside from intermodel comparisons, the field data from the Roda Sandstone serve as a benchmark for evaluating the performance of numerical models.

4.1. Surface features

The analysis of surface features begins with elevation maps of the delta models to depict their morphology. The analysis is then followed by other metrics, namely delta area, delta length, and active pixel counts, which together illustrate the distribution of sediments and the pattern of delta growth in the simulated process.

4.1.1. Elevation map

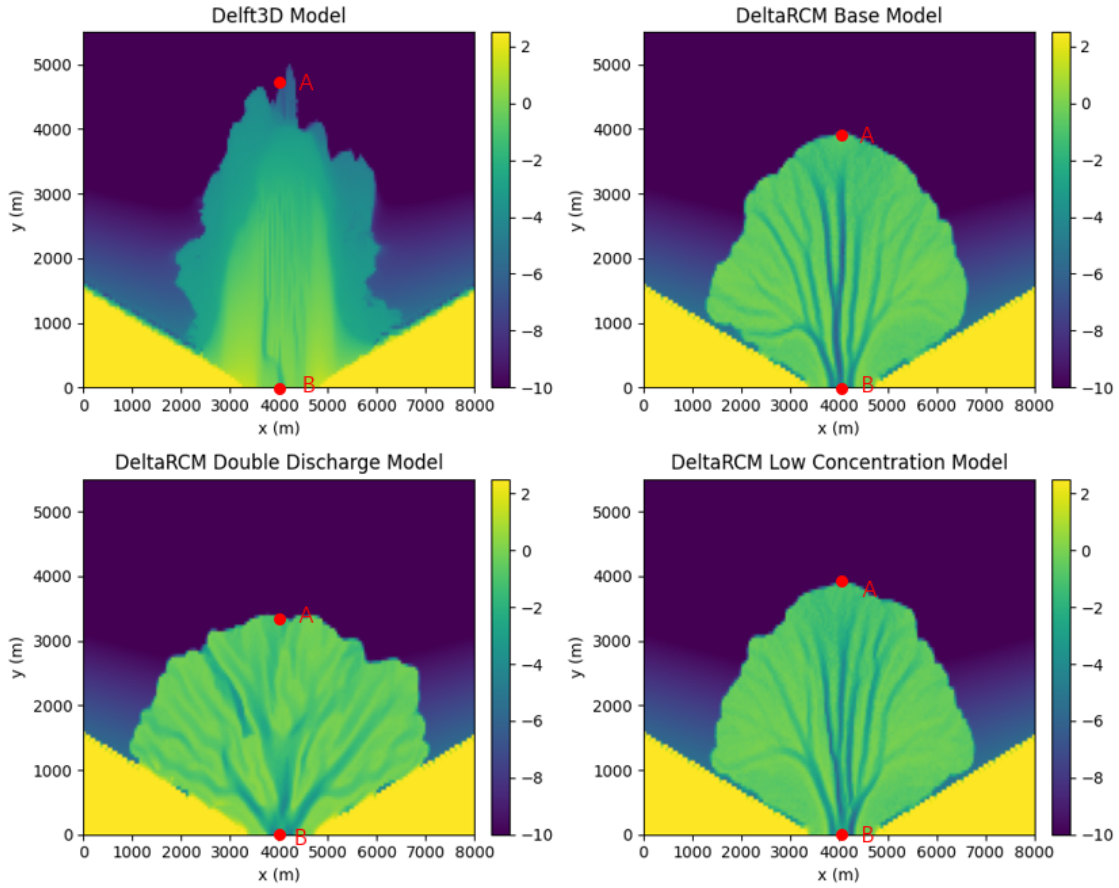

Figure 4.1: Elevation map of delta models. A and B indicate the centerline of the delta for calculation in the delta length in Figure 4.3 and cross-sections in Figure 4.12.

The elevation map presents planform geometry. Delft3D shows an elongated delta in Figure 4.1, with dimensions of 5km in length (y) and 4km in width (x). Unlike all the DeltaRCM models, the Delft3D model lacks well-developed distributary channels and exhibits a rough shoreline. The highest elevation occurs in the central part, where a larger subaqueous delta is present. The model overall shows a less channelized distribution of sediments, consistent with constant tidal and wave forcing rather than solely channelised sand distribution (Deltares, 2024).

In contrast, the DeltaRCM Base model (Base model) generates a more semicircular fan-shaped delta (Figure 4.1), with a length of 4km (y) and a width of 5km (x). It clearly shows the main distributary channels with several minor branches. Compared with the Delft3D model, the Base model shows a delta with smoother shorelines and a more homogeneous elevation of 0m, indicating a more river-dominant delta with stable flow paths and continuous sediment supply.

Unlike the Base model, the DeltaRCM Double Discharge Model (Double Q model) produces a rectangular footprint of a delta with a length of 3km (y) and a width of 6km (x) (Figure 4.1). Instead of showing strong channelised features with continuous elongated channels, the Double Q model presents a more discontinuous morphology, characterised by fragmented flow paths and wider and slightly shallower channels (1-2 meters shallower). The elevation is similar to the other models The morphology indicates that, under high discharge, the system favours lateral sediment dispersion rather than continuous channel development.

DeltaRCM Low Concentration model (Low C model) shares resemblance with the Base model, with similar shape, dimension, shoreline roughness and the elevation of the delta plain (Figure 4.1), but the channels extend further into the basin and are more concentrated towards the delta front. It suggests that, at low concentrations and thus low sediment load, the development of channels is slower via aggradation.

The morphological differences in those maps primarily illustrate the sensitivity of the delta system and channel distribution to discharge and sediment concentration in DeltaRCM. Similar findings upon sensitivity tests are also recorded for the Delft3D model (Deltares, 2024). The deltas are of similar dimensions but still differ in channel distributary patterns. The Double Q model generates a more rectangular delta with enhanced lateral sediment dispersion, while the Low C model promotes channel extension through slower aggradation.

4.1.2. Area

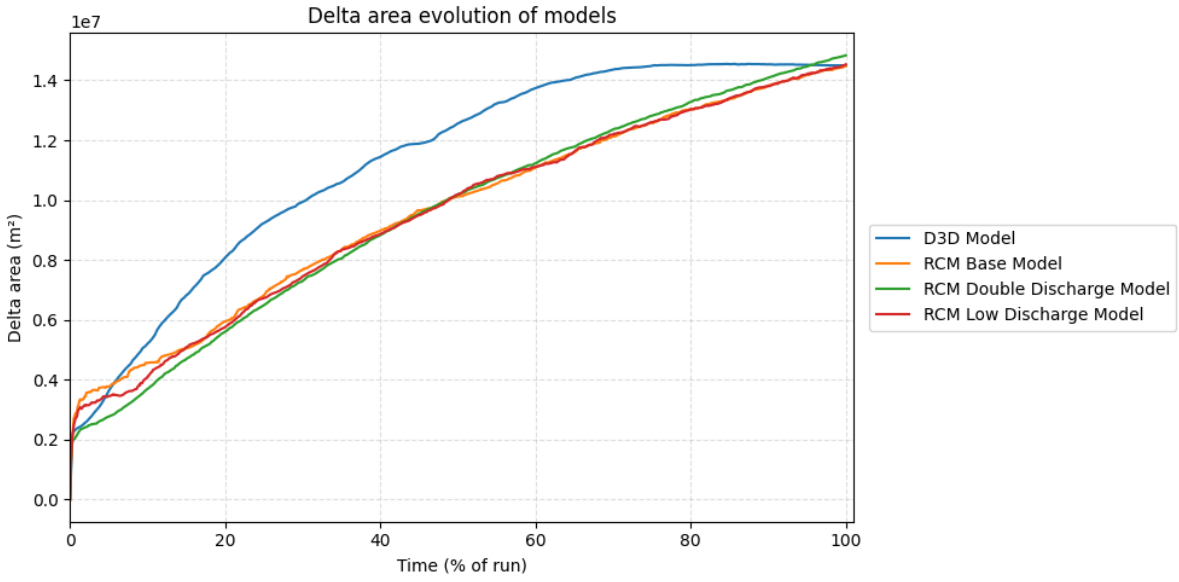

Figure 4.2: Delta Area Growth of models

The area of delta growth provides a quantitative understanding of the delta planform evolution. Delta-area growth of the Delft3D model increases rapidly during the initial 20% of the run, then slows after 50% of the model time. It reaches a plateau at 70% of the run, when the total area of the model is about $1.4 \times 10^8 m^2$. The slowing of the delta growth rate is consistent with the linearly decreasing discharge in the Delft3D setting (Deltares, 2024), as progradation becomes more difficult with reduced sediment supply. By 70% of the run, the feeding channels can no longer deliver sufficient sediments to feed shoreline growth. The rate of change of delta area growth, shown as the slope of the plot, can be explained using the formula by Wang et al (Wang et al., 2025)

$$dA_{delta}/dt \propto Q_{river} - A_{delta} * SLRR. \tag{4.1}$$

where d_{delta}/dt is the delta area change over time, Q_{river} is the fluvial sediment supply, $SLRR$ is the sea level rise rate.

From the Equation 4.1, the rate of delta area growth is proportional to the difference between river discharge and delta area multiplied by the sea level change rate. Since the sea-level rise rate has an equivalent effect to subsidence in the Delft3D model, dA_{delta}/dt decreases as discharge declines when the subsidence rate remains constant (equivalent to sea-level rise), which explains the decrease in area growth rate.

In contrast, all DeltaRCM models exhibit similar patterns of area growth. The delta area increases rapidly at 10% of the run, then the rate slows, but the delta continues to grow towards $1.4 \times 10^8 m^2$. The slowing of the growth rate can be understood as seaward delta growth requires increasing sediment supply to fill the increasing accommodation space.

During the first 10% of the run, the Base model has the largest area of $0.4 \times 10^8 m^2$, while the Double Q model has the smallest delta of $0.3 \times 10^8 m^2$. As delta progression continues, the area growth rate slows under constant sediment discharge, and curves begin to overlap. By the end of the simulation, the Double Q model has the highest value of $1.42 \times 10^8 m^2$, which is slightly higher than the other two models. Still, the 1% difference in delta area between DeltaRCM models is negligibly small relative to the total area and cannot indicate differences in the delta-area growth pattern under different discharge or sediment concentration among DeltaRCM models.

Overall, the Delft3D model and the DeltaRCM models exhibit distinct delta-area growth patterns due to different discharge conditions. In Delft3D, the correlation between declining discharge and the corresponding sediment input limits delta progradation, leading to a more significant decrease in the delta area growth rate. DeltaRCM maintains constant sediment input at each timestep, and the growth rate slows as accommodation space increases. The comparisons highlight that both models reach a similar final surface area using identical total sediment input and accommodation space, and the growth pattern is governed by the sediment supply regime in Delft3D when hydrological feedback also regulates the progradation in the Delft3D model.

4.1.3. Length

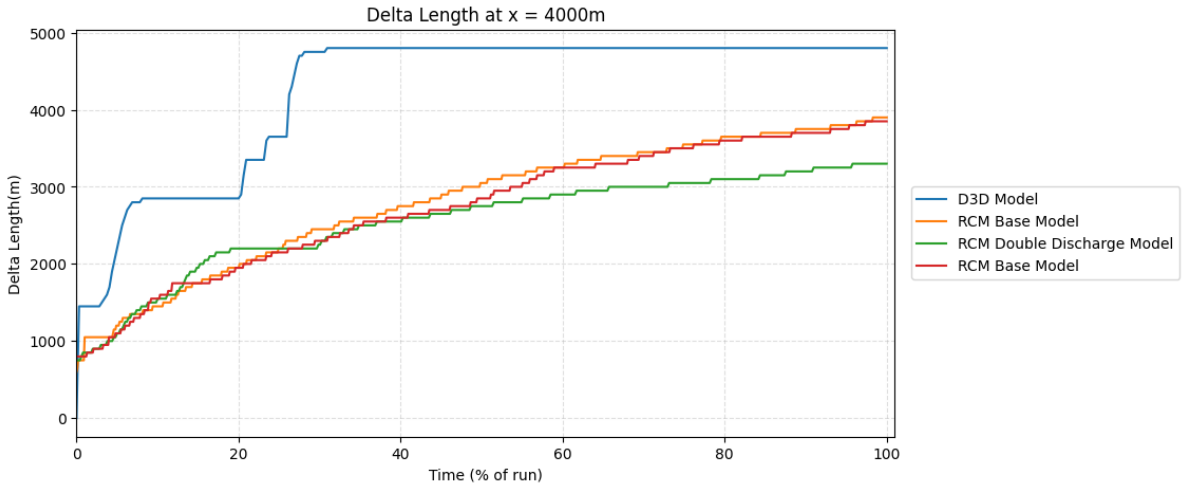

Figure 4.3: Delta Length at the cross section AB from Figure 4.1

Figure 4.3 focuses on the seaward growth of the delta front and provides temporal information on sediment distribution at the distal delta evolution. Along the cross-section, the Delft3D model produces the farthest delta front, roughly 5km, with a staircase growth pattern. The first staircase begins at 15% of the run when the delta front reaches around 3km, and more frequent jumps occur between 20% and 30%. The delta length continues to grow until the plateau at 5km, around 30% of the run. The step indicates rapid progradation in the seaward direction as lobes form, while the plateaus generally indicate the intervals when delta lobes grow on other locations after avulsion (Figure 4.4). For the final plateau, which starts at 30% of the modelling time, sediment supply is reduced due to lower water discharge and channel avulsions, making the delta prograde in other directions rather than along the centerline during this period.

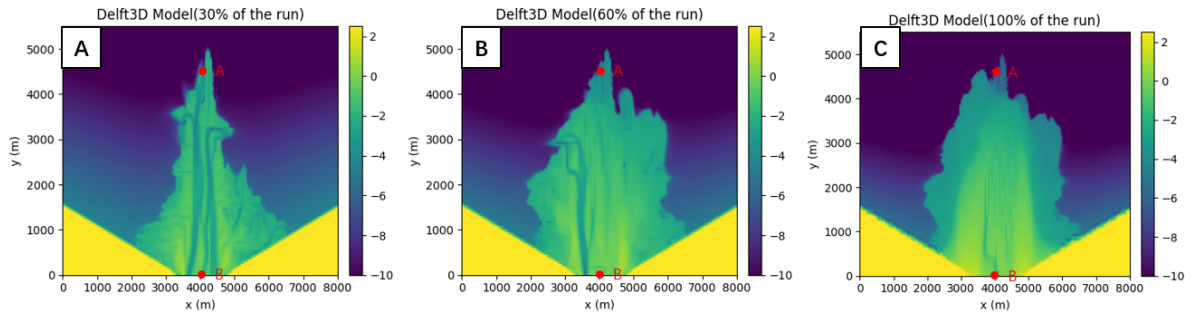

Figure 4.4: The elevation map of the Delft3D model at 30% (A), 60% (B) and 100% (C) of the run. A. B indicates the centerline where the delta length is measured. Between A and B, there's no change in the length of the delta after 30% of the run.

All DeltaRCM models show smoother, more continuous delta-length growth than the Delft3D model, with negligible jumps (greater than 0.5 km) or plateaus throughout the simulated process. The Base model and the Low C model follow a similar trajectory, reaching a similar length of 4km by the end. Both increase steadily throughout the delta's growth, indicating continuous progradation with limited large-scale avulsions. Between 30% and 60% of the run, the Base model first extends 0.5km further than the Low C model. Low C model then catches up gradually, consistent with the positioning and development of feeding channels for both models in Figure 4.5, as the Base Model develops a more mature feeding channel network that is closer to the centerline, whereas the Low C model only develops mature feeding channels during the mentioned 30% to 60% period, allowing it to catch up later in the run.

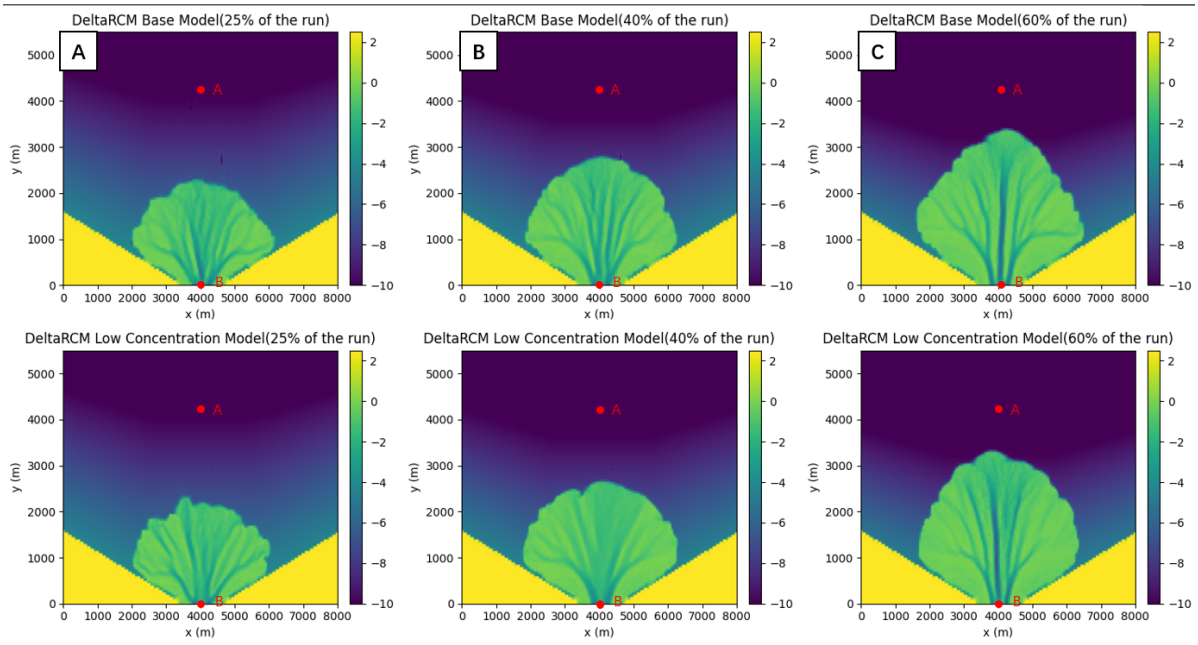

Figure 4.5: The elevation map of the Base model and the Low C model at 30% (A), 50% (B) and 60% (C) of the run. A. B indicates the centerline where the delta length is measured, and also the final length of the delta.

The Double Q model shows a different evolution pattern, with initial rapid growth until a 'stair-case' at 20% of the run, with a length of 2km. The delta continues to grow steadily at a lower rate from 30%, as the plateau suggests the establishment of early channels, where the high-discharge system forms wider channels and favours lateral sediment spreading, leading to a more expansive delta than in all the other models.

The delta length findings align with the dimensions and processes shown in Figure 4.1. Delft3D models

produce deltas that allow large-scale avulsion, whereas DeltaRCM models produce stable, continuous delta progradation with no major avulsion events.

4.1.4. Active deposition cells

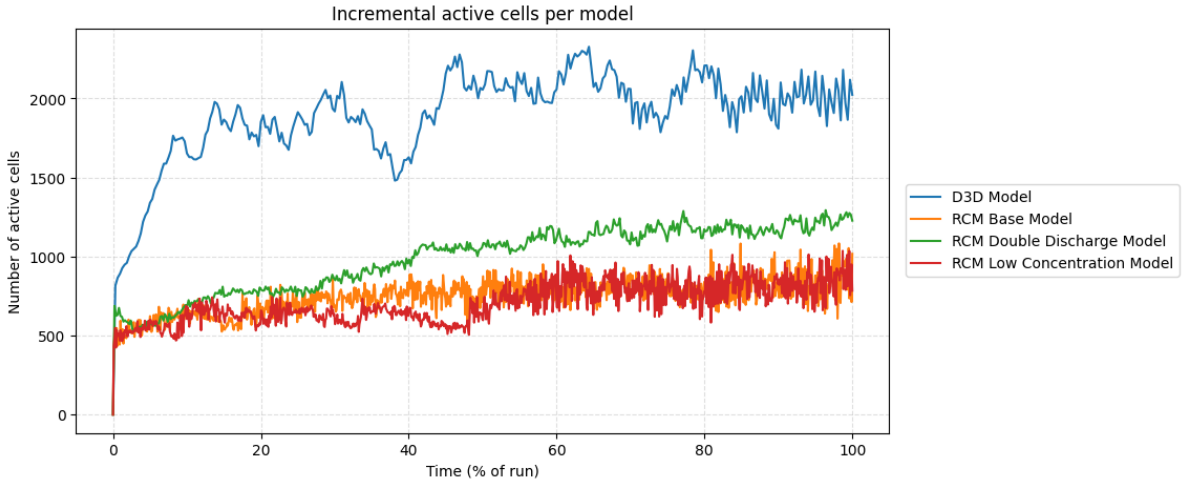

Figure 4.6: Active deposition cells count of models

The number of active deposition cells counts the cells where deposition of at least 0.001m occurs. In the Delft3D model, the number increases rapidly at the start of the run, then undergoes strong oscillations throughout the run. From start to around 35% of the run, the first phase fluctuates between 1500 and 2000 cells, then declines sharply. Around 70% of the run, the number increases, with a higher frequency of value variation, peaking at 1700-2200. The fluctuating pattern shows that the Delft3D model is more event-driven, as periods of number increase correspond to new lobe formation and avulsion. In contrast, a decrease in the number indicates that channels are merging or being abandoned, as visible in Figure 4.7. By tracking the spatial distribution of active cells and combining with the elevation map, as sediment discharge decreases towards the end, avulsions tend to occur frequently near the inlet, forming shorter channels that extend laterally due to relatively enhanced tidal and wave effects. Similarly, there's deposition in the distal delta due to wave or tidal reworking (Figure 4.8).

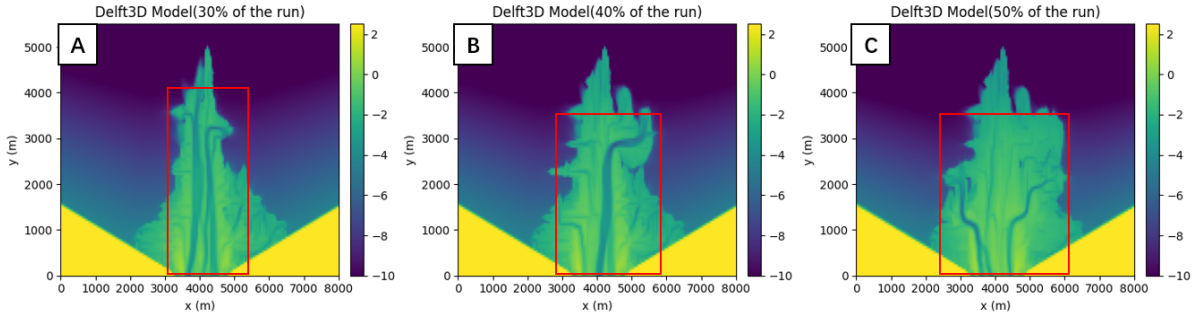

Figure 4.7: The elevation map of the Delft3D model at 30% (A), 40% (B) and 50% (C) of the run. The red squares from A and B capture channel merging, and accordingly, the formation of a new channel from B to C

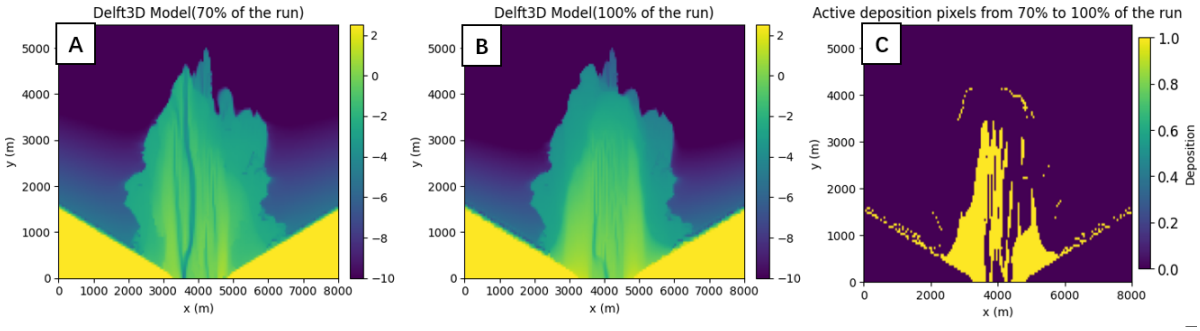

Figure 4.8: The elevation map of the Delft3D model at 70% (A), 100% (B) of the run. (C) records the map view of active depostion cell distribution during this period

Compared with the Delft3D model, all DeltaRCM models exhibit more stable active deposition cell counts and smoother temporal growth. In the map view, the spatial distribution of active deposition cells in the DeltaRCM model captures both delta progradation and channel-migration deposits. The Double Q model records the most significant increase, from 500 to 1200 by the end, as it generates a slightly bigger delta with a broader flow network, as shown in Figure 4.2. The Base model also shows an increasing number of active cells, starting similarly at 500 and increasing to around 1000, with strong oscillations throughout the process, suggesting that the delta continues to prograde and that avulsion occurs primarily in localised channels, while the main feeding channel remains relatively stable.

The Low C model has a similar range of active cells to the Base model, but it shows a gentle drop from 700 to 500 cells at 50% of the run, followed by a rapid recovery with strong oscillations from 500 to 1000 cells. The gentle drop indicates small-scale channel merging during channel development in Figure 4.5, and the magnitude of oscillation is comparable to the final phase of the Delft3D model and is likely to indicate small-scale channel avulsions near the river mouth.

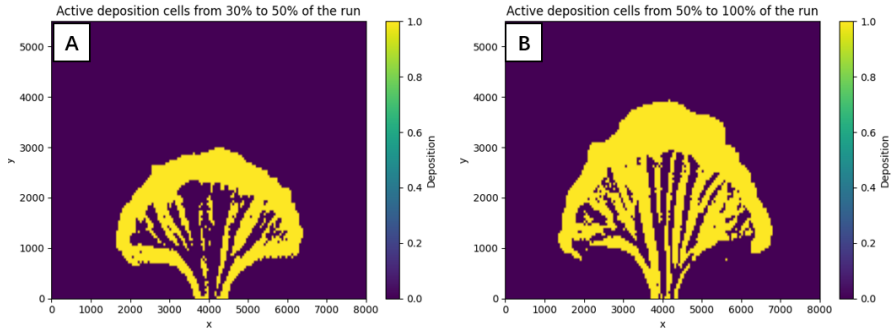

Figure 4.9: Map view of active deposition cells of the DeltaRCM Low Concentration Model. The first plot is active deposition cells between 30% and 50% of the run(A), corresponding with the elevation map (Figure 4.5) and the second plot records the active deposition cells (B) from 50% till the end

The active-cell analysis quantifies the magnitude of morphological change and reflects patterns consistent with elevation, area growth and delta length evolution. The Delft3D model captures large-scale avulsions associated with declining discharge, while the DeltaRCM model represents more gradual delta progradation through stable channel growth.

4.2. Subsurface metrics

The analysis of subsurface metrics builds upon the surface-based analysis by illustrating how depositional structures are preserved in the subsurface. The analysis begins with delta-volume growth over time, enabling a deeper look at the relationship between sediment input and delta evolution. This is followed by preserved sand thickness and net-to-gross ratio (NTG), which are key indicators for potential reservoir applications. Together, these analyses provide insight into the subsurface expressions for

both models and provide a basis for field comparison.

4.2.1. Volume

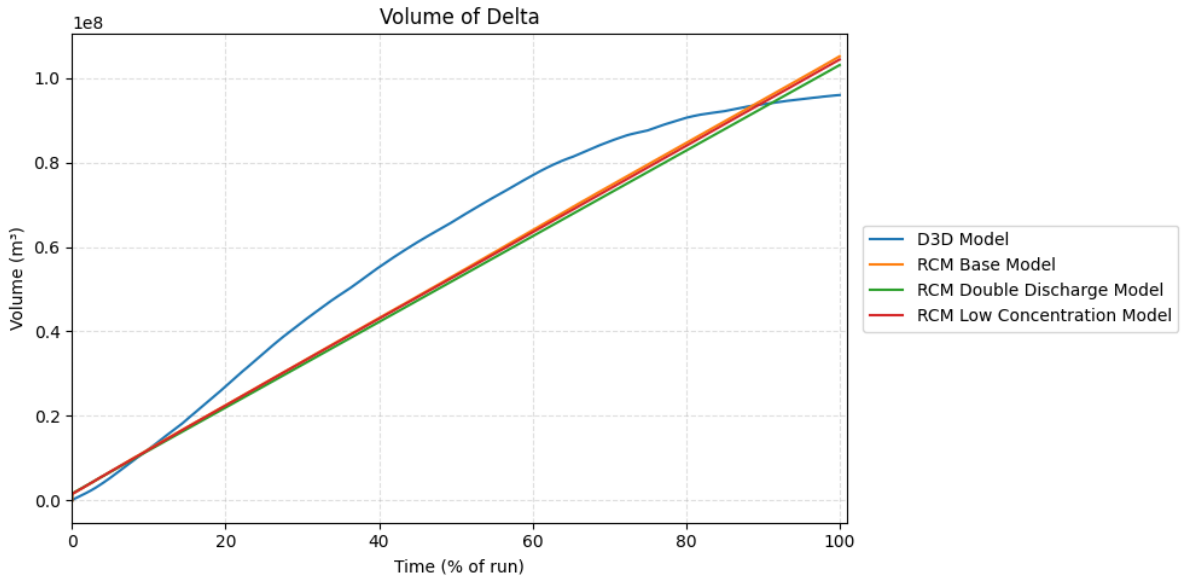

Figure 4.10: Deposited volume of delta models

All models are expected to have similar total deposited volumes, as each is forced with a comparable cumulative sediment input volume (1% rounding error). The Delft3D model shows a rapid increase during the first 30% of the run, then the growth rate slows after 50% of the run and continues to decrease until it reaches a volume of $1 \times 10^8 m^3$. The growth pattern is consistent with linearly decreasing water discharge, as net deposition slows with reduced sediment input.

The volume of all DeltaRCM models follows a linear increase to $1 \times 10^8 m^3$ by the end of the run, which indicates that the volume of sediment supplied at the boundary matched the volume deposited. The difference in volume growth patterns is negligibly slight among DeltaRCM models, indicating that cumulative volume growth is not sensitive to variations in discharge or sediment concentration under constant supply.

Despite similar total sediment volumes, the difference between the volume growth pattern for the two models is more likely from the model set-up, or specifically the sediment supply scheme, rather than the modelling methods. Deposition under linearly decreasing sediment discharge leads to a growth pattern that increases fast and then slows down, while constant sediment discharge enables continuous linear growth of delta volume.

4.2.2. Sand Thickness & NTG

With a similar amount of sediment input, the plots of sand thickness and NTG to show the spatial distribution of the sand to assess reservoir quality for further applications. The sand thickness map and NTG are shown per model to allow comparison of depositional patterns and heterogeneity (Figure 4.11).

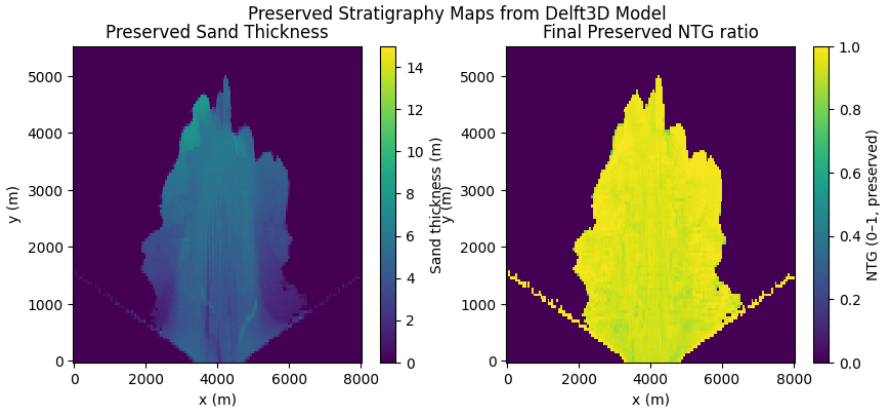

(a) Delft3D Model

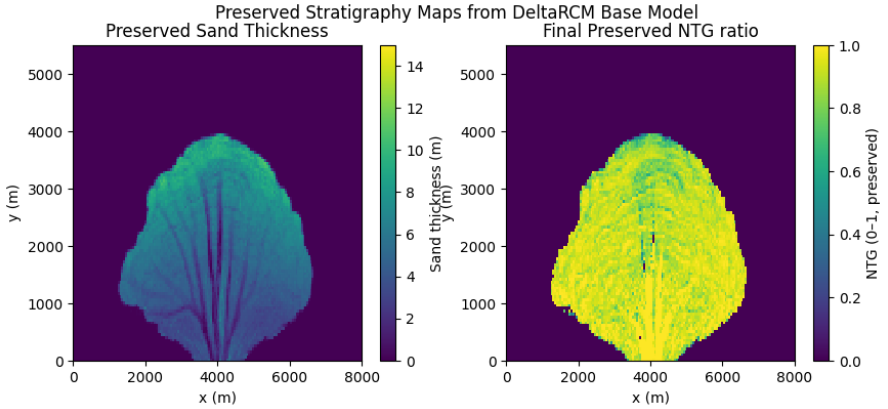

(b) DeltaRCM Base Model

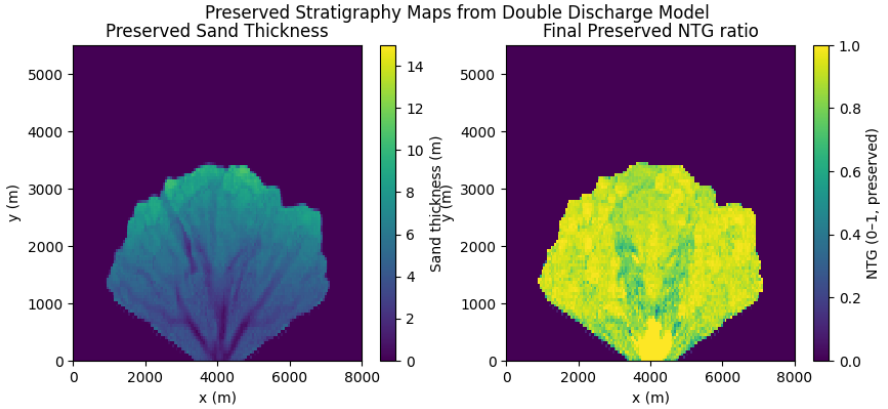

(c) DeltaRCM Double Discharge Model

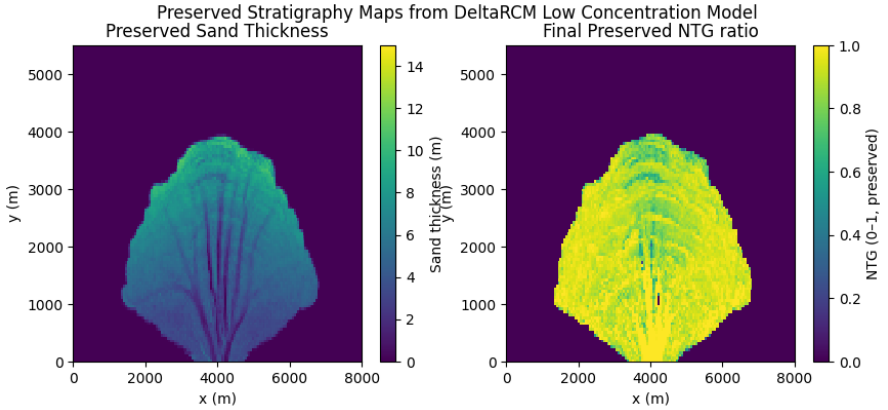

(d) DeltaRCM Low Concentration Model

Figure 4.11: Preserved stratigraphy maps showing (left) sand thickness and (right) final NTG for (a) Delft3D, (b) DeltaRCM Base, (c) DeltaRCM Double Discharge, and (d) DeltaRCM Low Concentration models. All maps share identical color scales and domain dimensions for direct comparison.

Sand thickness in the Delft3D model (a) ranges mostly between 3m and 10m, with thicker deposits along the central axis and thinner deposits towards the delta margins. The sand distribution is laterally continuous and less channelised than the DeltaRCM results. NTG is relatively homogeneous across the entire deposit, indicating diffusive sedimentation and a weaker river-dominant pattern.

DeltaRCM models generally show a stronger river-dominant pattern, with deep channel incisions rather than avulsions and lobe switching. In the base model (b), sand thickness increases gradually seaward from 2m near the inlet channel to around 10m toward the delta front. The sand distribution is highly channelised, with a typical channel-fill thickness of 2m, increasing to thicker lobe regions. NTG values are highest (0.7-1.0) along the channels and the mouth bar, but lowest in the floodplain, indicating a clear difference between sandy and muddy depositional zones.

Under double discharge, the Double Q model (c) develops wider and thicker channels, with the sand-bodies extending mainly to 3km into the basin. Unlike the Base Model, the overall thickness changes little seaward, suggesting enhanced lateral sediment transport in the channels. NTG value remains high in the main river channels but noticeably lower in the floodplain, reflecting a more sand-dominant deposit under higher discharge.

The Low C model (d) has a similar distributary pattern to the Base model, with slightly thinner sand bodies. The NTG pattern shows a more prominent band of interfingered high- and low-NTG zones that extends from 2km to 4km in the delta. The alternation between high and low NTG indicates the slow rate of delta progradation under low sediment concentration. Low NTG reflects the presence of the muddy delta front, which will shown in the following section.

Overall, the sand thickness and NTG maps show that Delft3D generates more uniform delta deposits, when DeltaRCM models have more channelised architectures. It is worth noticing that it only categorizes two classes, namely sand and mud, whereas in Delft3D it has five sediment categories and might show more variabilities in grainsize and lead to further heterogeneity. The findings are consistent with surface morphology patterns described earlier and emphasise how discharge and sediment concentration can affect the internal heterogeneity of deltaic deposits.

4.3. Field comparison

The following section compares the Delft3D and DeltaRCM models with Roda X field observations. The focus is on the cross-section and synthetic well logs extracted from DeltaRCM. When relevant, the Delft3D model's features are described qualitatively, but detailed cross-sections and logs are not shown.

4.3.1. Dimension

The dimensions of the delta models and the Roda X field data are presented first in Table 4.1.

Name	Length (km)	Width (km)	Thickness (m)
The Roda X (Leren et al., 2010)	1.3	1.5	5 - 20
Delft3D model	5	4	3 - 10
Base Model	4	5	2 - 10
DoubleQ Model	3	6	2 - 10
LowC Model	4	5	2 - 10

Table 4.1: Dimension of delta models and the Roda field data

Both the Delft3D and DeltaRCM models follow the Deltares concept model for the dimension of the model. The concept model is expected to generate a delta that is approximately 4km wide and 5km long, with a maximum thickness of 15m (Deltares, 2024). In contrast, Roda X field data shows a significantly greater thickness (5 - 20m) but smaller areal extent (1.3 ×1.5km) (Joseph et al., 1993; Leren et al., 2010). However, the reference model is chosen as it can reproduce the depositional patterns and architectural elements for Delft3D (Deltares, 2024). Moreover, the planform dimension of the Roda X in

field data is limited by outcrop and field data availability, so that the location and distribution of individual paleochannels and the progradation direction of sublobes remain uncertain despite existing studies on schematic average paleoflow direction (Joseph et al., 1993; Crumeyrolle et al., 1992; A. W. Martinius, 2017). Nevertheless, the dimension of the Roda X in literature provides a valuable reference for model comparison.

In the Roda X outcrop, individual lobes and sublobes can be clearly identified, as the interval of channel abandonment and lobe switching is capped by carbonate-cemented layers, more precisely defined as hardground bioclastic sandstones (Leren et al., 2010; A. W. Martinius, 2017; Alghamdi, 2023). In contrast, both Delft3D and DeltaRCM models lack carbonate deposition in the model, so such episodes of river evolution are separated by a time lag in the deposits as visible in Figure 4.12. A similar process with low or no clastic sediment input can be represented by the time-lags, which indicate periods of very low or no deposition in the original progradation direction. Therefore, the time-lags provide a proxy for the process of defining sublobes.

In the DeltaRCM simulation, the delta progrades without undergoing large-scale avulsions. Consequently, the blocks of depositional units are deposition of channel incision and subsequent infill rather than river avulsion.

The dimensions of depositional units of DeltaRCM are measured from the dip-section extracted from the DeltaRCM model cross-section in Figure 4.12 and shown in Table 4.2. In contrast, sublobes in the Roda are identified based on the outcrop, especially based on carbonate hardgrounds formed during channel abandonment (A. Martinius and Molenaar, 1991). A similar process is represented by time-lags in DeltaRCM models, as explained.

Still, the sublobes (depositional units) in Deft3D and DeltaRCM are reference groups based on cross-section geometry and deposition time rather than a stratigraphic match to the field data in Table 4.2.

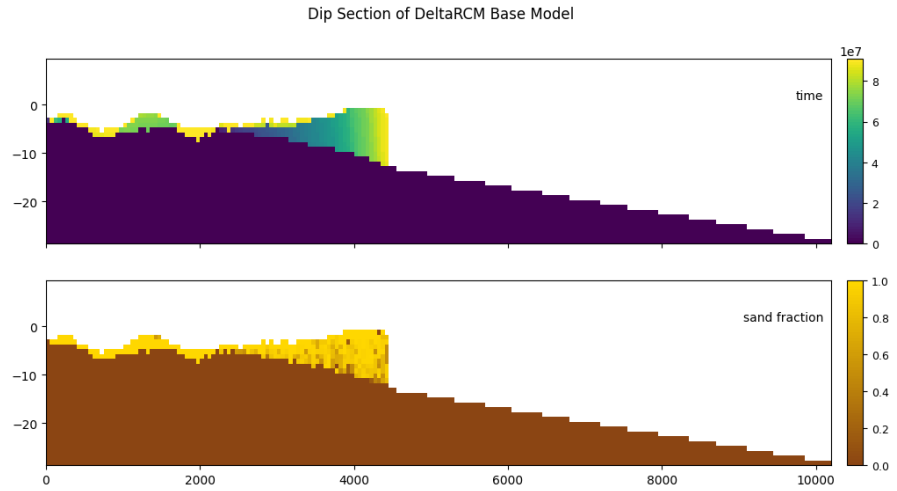

(a) Dip section of DeltaRCM Base Model

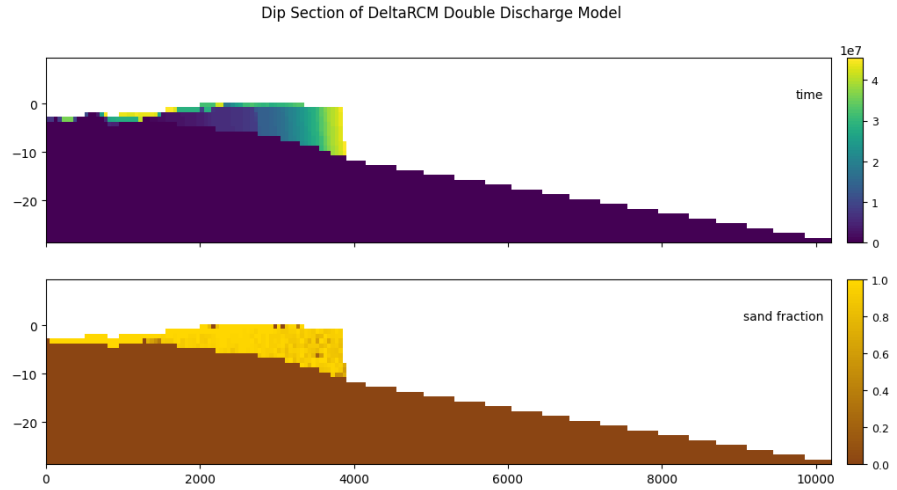

(b) DeltaRCM Double Discharge Model

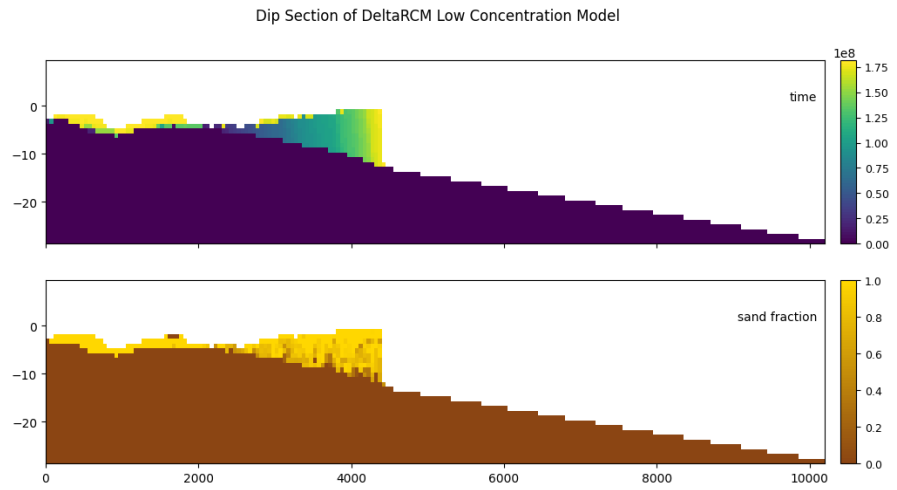

(c) DeltaRCM Low Concentration Model

Figure 4.12: Dip section of DeltaRCM Models using Sandplover. The cross-sections are taken in the centreline A-B of the delta models in Figure 4.1. The plots for each DelftaRCM model show the stratigraphic evolution (Top) and sand fraction (Bottom) of the delta.

	Field data	Delft3D Model	Base Model	DoubleQ Model	LowC Model
Depositional units (L + T)	1.2 km + 10 m 1.5 km + 10 m 1.6 km + 15 m 1.4 km + 12 m 0.8 km + 20 m	1.0 km + 2 m 3.0 km + 4 m 2.5 km + 2 m 2.5 km + 6.9 m 2.5 km + 1.4 m	1.5 km + 5 m 1.5 km + 6 m 1.7 km + 2 m	0.5 km + 2 m 1.2 km + 7 m 2.5 km + 7 m	1.0 km + 3 m 0.5 km + 2 m 2.3 km + 7 m 0.8 km + 3 m
Total length	1.7 km	4.8 km	4.1 km	4.0 km	4.1 km
Total thickness	12–20 m	3–10 m	2–10 m	2–10 m	2–10 m

Table 4.2: Dimensions of depositional units among models. L and T represents maximum length (km) at the cross-section and the thickness (m). The depositional units from both models serve as references rather than exact stratigraphic equivalents to the Roda X sublobes. The Roda field data is measured from Leren et al., 2010 and A. W. Martinius, 2017; A. Martinius and Molenaar, 1991. Delft3D results are measured from Deltares, 2024.

In all DeltaRCM models, deposition ages young basinward, indicating continuous delta progradation into the basin. In the DeltaRCM model, it appears as one main lobe overlain by small, discontinuous sediment bodies with distinct age breaks. The dominance of thin, discontinuous sandbodies and the sharp age break are interpreted as channel incision fills. Erosional surfaces are especially evident in the DeltaRCM Base and Low C model, as the topography slope and sediment deposits are truncated. Except for the Double Q model, where mud is more present in the delta top, other models have mud deposits mainly at the bottom of the delta, consistent with the deposition of finer sediments during progradation. The Double Q model, however, shows a steadier progradation pattern with incised channels on the delta top.

In contrast, the Delft3D model exhibits more laterally extensive sediment units with distinct deposition times. Depositional age decreases with decreasing burial depth and increasing distance from the inlet. The major part of the delta (delta front) was deposited in the first one-third of the simulation, and the deposition rates decreased due to reduced discharge, similar to what is depicted in Figure 4.10, forming a thinner delta top deposit (Deltares, 2024). An erosional contact can be observed between the channel deposits and the overlaying young delta top deposits, which suggests the enhanced tidal reworking (Deltares, 2024). The continuity and geometry suggest the deposits are part of the delta front (Deltares, 2024).

4.3.2. Logs

Four synthetic logs are taken in the DeltaRCM Low C Model, showing the clearest pattern of channel incisions (see Figure 4.13). The logs are taken at locations referenced to the Delft3D model and field data to show the distal, medial, and proximal parts of the delta (Leren et al., 2010; Deltares, 2024). The correlation is shown in Figure 4.14.

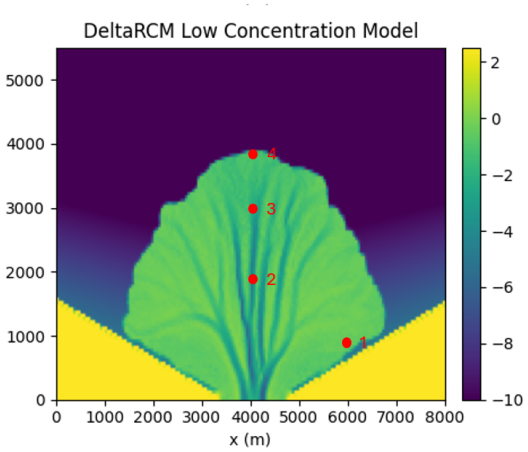

Figure 4.13: Location of virtual logs in DeltaRCM Low C model

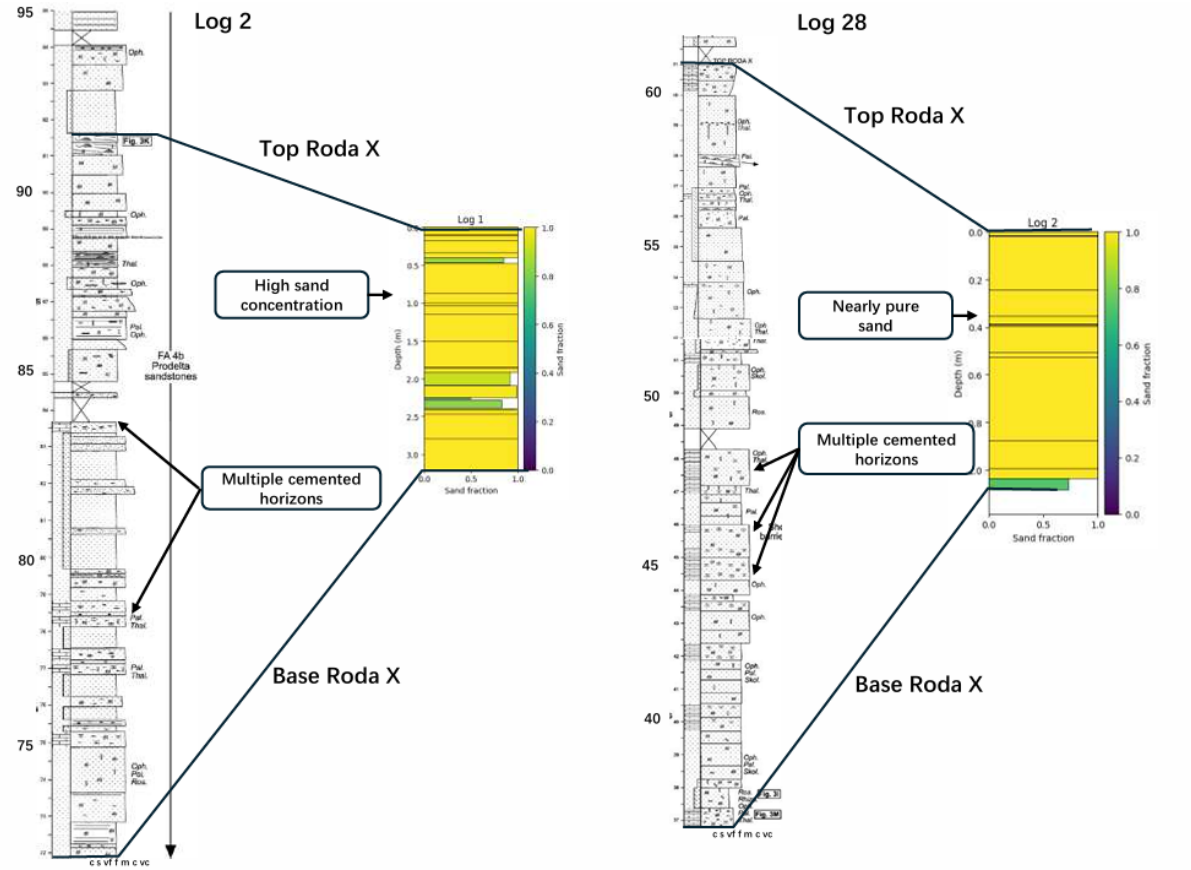

(a) Comparison between field logs 2 and 28 (Leren et al., 2010) with DeltaRCM logs 1 and 2

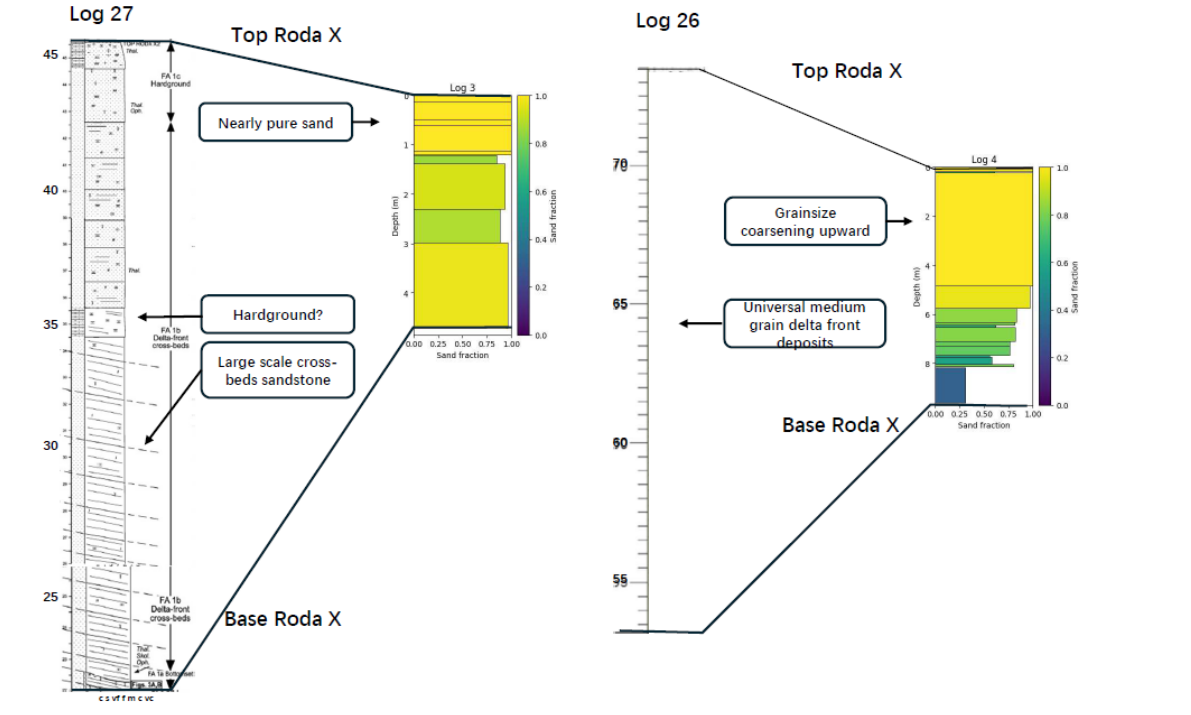

(b) Comparison between field logs 27 and 26 (Leren et al., 2010) with DeltaRCM logs 3 and 4

Figure 4.14: Comparison between Roda field logs and DeltaRCM logs. Log 26 is only presented in the unpublished Delft3D model report and left out in the figure (Deltares, 2024). The axes of field logs are simplified and edited for visualisation.

Across all locations, the modelled logs show a comparable stratigraphic trend to the field data and to the Delft3D logs. This part will focus on the description of trends in logs and the processes captured in the models, and the detailed mismatches will be analysed in the following discussion chapter. The logs are analysed by distance from the inlet, and the comparison will focus on overall thickness, sand-mud proportions, vertical sand-fraction trends, and the presence of special surfaces.

Two consistent discrepancies are observed in the preserved stratigraphy. The first is the lack of carbonate sediments in the models, as both numerical models (Delft3D and DeltaRCM) can partially reproduce the siliclastic composition of the Roda Sandstone. Still, bioturbation and cemented horizons, which are widely present in the field logs (Leren et al., 2010), are absent. These features indicate diagenetic processes and biological activities in the formation of the delta and may impact the reservoir's characteristics for further applications (A. W. Martinius, 2017). The second mismatch is that the deposit thickness is thinner than the field data, as explained in Table 4.1. It is also notable that DeltaRCM includes only sand and mud in the sediment system, therefore simplifying the grain-size comparison.

Log 1
Log 1, located near the landward boundary, is dominated by high sand fractions over 3 m deposits. Between 0.5 and 2.5 m, there are several thin layers with slightly lower sand fraction (around 0.7), and the main body of the log consists of pure sand.

The Delft3D log shows a similar sediment thickness (4m) with thinner deposits on top. The grain size of the Delft3D log is similarly homogeneous and mainly consists of medium sand, with a subtle decrease in grain size in the top 1m (Deltares, 2024).

By contrast, The Roda field log (19.5m) comprises thicker, more heterogeneous deposits that mainly consist of medium sandstones with trace fossils, several cemented horizons, and conglomerate lags throughout the whole log.

Both models reproduced the sand-dominant feature in the log. The Delft3D log captures thin layers of variable-grain-size deposits near the top, comparable to the small vertical variations in the field. DeltaRCM produces a more uniform sand-rich deposit.

The high sand concentration across all logs indicates high-energy deposition in the proximal setting. In the Roda field log, these heterogeneous sandstones are interpreted as wave-modified prodelta sandstones deposited below the fair-weather wave base (Leren et al., 2010). Both models simplify the deposition process and fail to capture the complexity of lithology and depositional environment, as the DeltaRCM model depicts a channellized, sand-dominant environment with one single sandbody in a high-energy environment, and Delf3D preserved minor vertical textural change due to wave reworking.

Log 2
Log 2 records deposits in the proximal part of the delta, with a thickness of around 5m, characterised by a uniformly high sand fraction of around 1. Similar to Log 1, the lower 0.5m comprises a slightly lower NTG layer (0.7).

The Delft3D model shows a thicker layer (9m) comprising alternating fine- to medium-grained sand layers (Deltares, 2024). Despite the subtle coarsening-up trend, there are frequent variations in the grain size with thin layers of coarse sand in the lower 6m. The upper 3m of the Delft3D model has uniform high sand content. No clear bounding surface or abrupt shift is visible.

Field log 28 records a 20m succession that is also sand-dominant. The grain size shows a subtle pattern of coarsening from very fine sand at the bottom to fine sand at 10m depth. Consequently, the upper 10m records a thinning upward trend from fine sand to very fine sand. In the lower 10m, frequent cemented horizons are observed.

Both model shows a thin, sand-dominant succession relative to the thicker, more heterogeneous field log. Delft3D captures grain-size variability and a uniform high-sand fraction interval. DeltaRCM gener-

ates a uniform, high sand-fraction profile at the proximal delta.

The field Log identifies the deposits as being in a spit-barrier environment, as they were heavily modified by wave resedimentation and reworking. Regular cemented horizons were also identified as they were off-axis and deposited along the coarse-grained delta (Leren et al., 2010). Comparing two models with field data, Delft3D depicts more clearly the change in depositional environment and the regular deposition and erosion patterns via variation in grain size. In contrast, DeltaRCM simplifies the process and generates a single sand body.

Log 3
At the medial location (Log 3), all logs show overall sand-dominant successions. Field log 27 records a total thickness of 23m, where the lower 25-35m of the log consists of large-scale cross-bedded medium sands. In contrast, the upper 35-45m interval comprises thin-bedded horizontal sands, capped by hardground deposits.

In the Delft3D model, the total thickness is about 11m, with a similar two-phases pattern, with a sand-dominant lower half (7 - 11m) overlain by thick finer-grained delta-top deposits with variations in grain size (0 - 7m).

The DeltaRCM log (Log 3) records a thinner layer (4m) that is uniformly sand-rich (sand fraction 0.8-1), with little internal variation and no identifiable bounding surfaces.

Both models reproduce the primary vertical sand trend as seen in the field, as the log consists of nearly pure sand. Delft3D also captures the two-phase pattern as observed in the Roda log, while DeltaRCM generates a more homogeneous, sand-dominant deposit. All three logs also show a subtle increase in sand content towards the top, representing a comparable upward coarsening or cleaning trend.

The logs reflect progressive progradation of the delta front as sandy facies advanced over finer prodelta deposits. The two-part structure in the field and Delft3D logs suggests alternating stages of rapid sand deposition followed by lower-energy sedimentation or partial reworking at the top of sediments. The DeltaRCM model exhibits channel-dominant features and lacks distinct internal boundaries, reflecting its simplified representation of sedimentary processes.

Log 4
Log 4, taken at the most distal location, records a 10 m deposit with a clear coarsening-upward succession. The sand fraction increases from 0.25 at the bottom, gradually to 1 at 5m and remains 1 to the top.

The Roda field log 26 is approximately 20m thick and consists mainly of medium-grained sandstones with limited fine sand. Moderate bioturbation is present throughout, and the sand fraction slightly increases upward, with the upper beds composed of bioclastic sandstone.

By comparison, the Delft3D log shows a thinner 10 m-thick sand-dominant interval, with the lower 6 m consisting of thicker, more homogeneous medium-grain sandy deposits, and the upper 4m contains variation in grain size from medium sand to fine sand.

All three logs show similarly high sand content at the top. DeltaRCM captures the coasening-upward trend in the distal delta, and Delft3D records the fast deposition of sediments in the equivalent area (Deltares, 2024).

The grain size change in the DeltaRCM log indicates a clear pattern of delta progradation as the sand-rich facies progrades over the muddy prodelta (Nichols, 2009), which is consistent with the delta front facies defined in the Roda Log 26. The log 26 indicates the delta front deposits, which were formed by wave resedimentation over a gently sloping fan (Leren et al., 2010). Delft3D shows similar processes. Both models illustrate comparable delta-front facies, with Delft3D showing a brinkpoint and DeltaRCM a more gradual progradational pattern without a clearly defined clinoform break.

From the previous analysis, both models are capable of creating deltas that are comparable in the sand fraction and overall architectural patterns to those observed in theRoda X. However, notable differences remain, mainly in the dimensions of deposits and the depositional processes each model represents. While Delft3D captures more detailed vertical variability and reflects wave reworking, DeltaRCM produces simplified, channelised sandbodies. A more detailed description and interpretation will be analysed in the Discussion.

5

Discussion

The results presented DeltaRCM simulations and the comparison with the Delft3D model and the Roda field data. The discussion summarises the performance of numerical models and identifies the possible source of intermodel differences. Based on the study, suggestions and improvements are proposed for future geological modelling for the Roda Sandstone Formation and general delta modelling using DeltaRCM.

5.1. Model performance overview

The Roda Sandstone represents an Eocene delta system deposited in a foreland basin setting. Field studies describe coarsening-upward successions with cross-bedded channel sandstones, wave-reworked topsets, and carbonate cementation. These sandstone bodies consist of smaller sublobes (A. W. Martinius, 2017). The focus of the research is to investigate whether DeltaRCM can produce a geological model with a similar stratigraphic structure to Roda X, with special emphasis on the hierarchy of lobes.

5.1.1. Capacities

Both models can generate lobate deltas with similar platform dimensions between DeltaRCM and Delft3D. Under the high-sand fraction setup, both models generate predominantly sandy deltas. Under the boundary conditions used in this research, Delft3D models more effectively capture the hierarchy of lobes and sublobes in the preserved stratigraphy and can incorporate wave features into the model, generating wave-modified prodelta (Deltares, 2024). By contrast, DeltaRCM models emphasise channelised deposition with abundant incisions in the delta.

Comparison with well logs reveals that Delft3D also reproduces some of the environmental transitions observed in the Roda field data. At the landward location (Log 1), the Delft3D model incorporates the wave-reworked layers, which are similar to those observed in the Roda log. In contrast, DeltaRCM represents a simplified, channelised environment dominated by uniform sand deposition. In the proximal setting (Log 2), both models exhibit high sand fractions, reflecting high-energy channelised deposition; however, only Delft3D displays variations in grain size and erosional surfaces consistent with wave reworking. At the medial site (Log 3), both models reproduce the coarsening-upward trend and progradational stacking observed in the field, though at a smaller scale. At the distal site (Log 4), both models produced delta front deposits, and DeltaRCM generated a more gradual progradational pattern without a clearly defined clinoform break, which is closer to what was observed in the field.

Taken together, these comparisons suggest that DeltaRCM can capture the overall progradational morphology and sand–mud proportion of the Roda X. It can also generate different facies of the delta. Still, it lacks the hydrodynamic complexity required to reproduce reworking and facies transitions. Delft3D, by contrast, better approximates the mixed fluvial–wave depositional environment of Roda X.

5.1.2. Limitations

As discussed in the previous chapter, neither models match the outcrop's dimensions, and both lack bioturbation and cemented carbonate layers. However, the first issue is likely to be fixed by using a different model setup, including different subsidence rates and run times. The lack of lithologic variability can lead to overly homogeneous stratigraphy in the models. The progradation direction of both models is also not entirely consistent with schematic paleoflow reconstructions of the sublobes in Roda X (Crumeyrolle et al., 1992; A. W. Martinius, 2017). DeltaRCM models exhibit abundant channel incisions, which are rarely observed in the field.

Beyond geometric and sedimentological simplifications, both models only partially reproduce the depositional environments observed in Roda X. The field logs show a transition from wave-modified prodelta deposits in the landward areas to barrier and spit deposits to the delta front in the distal delta. Together with the conglomerate lags, carbonates and fossils, these features reflect the mixed fluvial–wave nature of the Roda delta, which neither model fully captures. Delft3D reproduces some of the upper-delta reworking but still underestimates the degree of lateral sediment redistribution and storm modification. DeltaRCM, in contrast, produces a more purely fluvial regime with smoother shorelines and lacks the hydrodynamic feedback required for realistic wave or tidal processes. As a result, both models simplify the environmental gradients along the delta and cannot fully replicate the vertical and lateral heterogeneity recorded in the field logs.

Additionally, DeltaRCM has only two sediment classes, which cannot capture the variation in grain size observed in Delft3D and field data. The simplification also leads to higher estimates of reservoir quality and poses challenges for subsurface applications. Besides, due to the lack of wave and tidal effect in the model, DeltaRCM cannot recreate the wave and tidal reworking that are present in the field data (Leren et al., 2010; Deltares, 2024).

One of the research questions concerns the possibility of recreating lobate structures using DeltaRCM. Under the current setup, DeltaRCM does not create a hierarchy of lobes and sublobes similar to those of the Delft3D model or the Roda field data, mainly due to the avulsion frequency represented in the model. In Roda X, lobes and sublobes were formed as the multiple channels underwent multiple avulsions and abandonment (Leren et al., 2010). In delta fans, most avulsions occur near the shoreline due to superelevation influenced by backwater length (Paola and Mohrig, 1996; Moodie et al., 2019; Gearon et al., 2024).

$$L_{bw} = \frac{H_0}{S_0} \tag{5.1}$$

where L_{bw} is the backwater length, H_0 is the water depth in the channel, S_0 is the bed slope of the basin.

In the DeltaRCM Base model, the chosen parameters yield a backwater length of hundreds of meters (Table 3.1). This indicates a subcritical flow where the gravitational forces dominate the system over inertia. Such a system tends to be more stable and is less prone to frequent avulsion. In DeltaRCM, bed elevation is dictated by water routing, which uses a smoothed scheme for large-scale water-surface calculation (Liang et al., 2015). Yet, on a localised scale, the simplification might dampen the sharp water surface and the resulting superelevation, and the backwater effect is not considered at that scale. This could explain why DeltaRCM was unable to generate models with avulsion under the current settings.

5.2. Understanding intermodel differences

DeltaRCM and Delft3D are fundamentally different models as described in the methodology chapter. In the current model setup, DeltaRCM inherits many adapted hydrological and morphological parameters from Delft3D (Table 3.1); however, the differences between models are still distinct and that can be attributed to a few major functional parameters.

5.2.1. Water discharge

As mentioned in the methodology chapter, this research could not use the same water discharge scheme as Delft3D due to DeltaRCM's instability under the current setup. The instability of DeltaRCM

is associated with the mechanism for lateral water dispersion, which is calculated as:

$$\gamma = g \cdot dx/u_0 \tag{5.2}$$

where g is the gravitational acceleration, dx is the grid resolution, u_0 is the flow velocity at the inlet, and γ is the partitioning parameter, routing by inertia and by free surface. For model stability, γ is expected to be in the order of 10^{-2} (Liang et al., 2015). In previous tests, the γ value can reach 2, and the model remains stable. However, if the boundary discharge is set to be the boundary condition of $250m^3/s$ under the current resolution of 50m, γ would increase to 4000, which would cause model failure.

To reduce instability at low discharge or low flow velocity, one approach is to use higher spatial resolution (dx = 10 - 20m), which will proportionally reduce γ. However, the higher resolution requires a longer runtime of 20-40 hours, similar to that of Delft3D. Thus, DeltaRCM will lose its advantage of being time- and computationally efficient, as it takes 5-10 hours to test the models in this research. Moreover, even at higher resolution, the γ value would remain large, and the model's robustness would remain questionable.

At the reservoir level, higher resolution would help capture subsurface variability. It is yet unclear whether the existing field data on well spacing (1 km) are valid to justify and explain the processes. Given DeltaRCM's time efficiency, multiple DeltaRCM models can be run to quantify uncertainties. Therefore, a more feasible strategy is to run additional simulations, analyse similarities and differences at lower resolution, and combine the uncertainties with a few fine-grid realisations (Durlofsky, 2005).

5.2.2. Sediment concentration

Delft3D and DeltaRCM use different sediment concentration schemes in the model; the former one uses mass concentration ($kg \cdot m^{-3}$) from Deltares, 2024, and DeltaRCM uses volumetric fraction (%) of the total water discharge. The two are related utilising Equation 5.3,

$$c_m = c_v \cdot \rho_{sand} \tag{5.3}$$

where c_m is the mass concentration, c_v is the volumetric fraction, and ρ_{sand} is the sand density (approximately $2650kg \cdot m/s^2$), which means the concentration of sediments in DeltaRCM is tens of times higher than the values used in the Delft3D model.

The higher sediment concentration in DeltaRCM results in a much larger sediment input rate under the same water discharge, which explains why building a delta of similar volume to the Delft3D model is much faster using DeltaRCM. The sediment concentration value $C_0 = 0.1$ is commonly used in DeltaRCM research (Liang et al., 2015; Moodie and Passalacqua, 2021; Hariharan et al., 2021). While it is possible to apply a much lower sediment concentration value to match that used in the Delft3D model and maintain model stability, the modelling time is expected to be 250 hours, which again undermines DeltaRCM's efficiency advantage.

5.2.3. Sediment types

Both models have a sand fraction of 90%, consistent with the field observation in Roda. However, the Delft3D model used six categories of sediments, ranging from mud to very coarse sand, which allows variations in the grain size distribution. By contrast, DeltaRCM simplifies the sediment types into sand and mud; thus, it is unable to capture the variation in grain size and adds difficulty for further subsurface applications.

5.2.4. Wave and tidal features

Delft3D sensitivity tests indicate that tidal amplitude, wave height and direction play only a medium to low impact on the morphology and stratigraphy of the Delft3D model (Deltares, 2024). In a sand-rich delta (90%), the penetration of tidal effects is limited mainly to the edge when the river dominates the depositional progress, as the dominant river flow push marine water seaward and confines the tidal influence to delta front or marginal channels (Bacopoulos et al., 2025), which also explains why tidal facies and reworking do not widely exist in the Delft3D model stratigraphy. Still, the Delft3D model can generate wave-modified deltas, as waves can redistribute sediments alongshore and offshore via

different transport directions. By contrast, such wave-driven features are absent in DeltaRCM and lead to a more strictly river-dominant delta.

5.3. Subsurface implications

For subsurface applications such as geothermal or CO2 storage, the connectivity of sand bodies and the internal heterogeneity are critical for fluid and heat transfer (Issautier et al., 2014). Both models have similar volumes and reservoir dimensions; thus, differences in flow behaviour will arise from their internal architectures. DeltaRCM has channelised sand bodies with a universally high sand fraction, which can enhance the connectivity between delta units and thus facilitate flow transport within the reservoir (Atlas, 2022). The abundant incisions can also promote vertical connectivity between the channel infills and the bed. However, channelised deposits and incision features are not observed in the field. The field log from Roda indicates layers of fine sand and very fine sand (Figure 4.14a), which cannot be reproduced in DeltaRCM, suggesting that DeltaRCM models would overestimate sandbody connectivity and provide an overly optimistic assessment of storage and transmissivity capacity. Moreover, the model lacks carbonate layers and bioturbation, which removes potential internal barriers or baffles that could influence flow. In DeltaRCM Base and Low C models, interfingering bands of high and low NTG can be observed in Figure 4.11, which can redirect and compartmentalise flow in the distal delta and therefore require careful well placement design.

In the face of similar uncertainties from missing carbonate layers, the Delft3D model generates a more laterally continuous delta with homogeneous, high sand fraction and thickness in Figure 4.11. In this case, reservoir connectivity is high, and well placement would have limited influence on the production. However, the spatial distribution of grain-size variability is not included in DeltaRCM. It is therefore omitted in Delft3D, which can lead to internal heterogeneity in the reservoir and affect reservoir quality.

Based on Roda field data, a study evaluated the feasibility of injecting CO2 into the formation and highlighted the effects of carbonate layers (Alghamdi, 2023). As laterally continuous, cemented layers disperse the flow path of CO2 and enlarge the contact area of the CO2 plume, it allows CO2 to be more efficiently stored in the subsurface. By contrast, discontinuous cemented layers cannot create a similarly effective trapping structure for CO2 (Alghamdi, 2023). These carbonate layers, however, are missing in both numerical models. To better understand the distribution of carbonate sediments, further fieldwork is needed.

5.4. Field data uncertainties

Current field data contains 4 logs measuring Roda X's lithology with a well spacing of around 1 km apart (Leren et al., 2010). By combining 1D logs and 2D cross sections, field data from Roda still has greater uncertainty in spatial constraints than the 3D geological model (Leren et al., 2010; Deltares, 2024). As a result, the areal distribution of facies remains uncertain, including the continuity of channel belts and delta-front deposits, the progradation direction and orientation of the delta, and the orientation of the mapped lobe geometry and sand body connectivity, where different facies correlations can lead to differences in mapped lobe geometry and sand body connectivity.

The variation in paleocurrent direction suggests a battle between fluvial and tidal currents in a supply-dominant delta (like Roda X), indicating complex flow and sedimentary dynamics during autocyclic lobe switching (Crumeyrolle et al., 1992; Xu et al., 2025). However, the extent of the tidal effect is not clearly evident in either numerical models or field data, making it difficult to quantify its influence on facies (Coll et al., 2013). Similarly, the true extent of the carbonate layers and the diversity in the extent of cementation are poorly known (Alghamdi, 2023), as explained in the previous sections. This also applies to wave reworking, as limited knowledge is known to the extent of wave modification to Roda X. Together, these uncertainties limit how precisely the field data can be used to validate modelled facies distributions and depositional processes.

5.5. Limitations

First, the current DeltaRCM model is primarily based on the reference Delft3D model rather than being built from scratch, which limits the dimension and magnitude of forcings. This model setup strategy does reduce workload on bathymetric data and forcings, but it already differs from the dimensions of the Roda X observed in the field.

Second, limited sensitivity tests were performed. All three tests focused on hydrological parameters, including sediment deposition and erosion. A broader sensitivity analysis is needed to evaluate the controlling factors in delta modelling and test the model's robustness. Starting with the accommodation space, such as the subsidence rate, would be feasible, as it only requires minimal changes to the existing model setup. Additional sensitivity tests can be conducted to explore the boundary conditions of DeltaRCM models, such as γ and sand fraction, to better understand the model's stability and physical interactions. For further exploration on the impact of the sediment routing scheme, changes can be made to the coefficients for sand and mud erosion (see Table 3.1) instead of the default settings from Liang et al.(2015).

Third, the current study lacked the conditions required to recreate a model more similar to the Roda X, including carbonate features and wave reworking, which need to be incorporated into the DeltaRCM model. Besides, the simplicity of sediment classes in DeltaRCM also hinders further grain-size comparisons with Delft3D and field data, which are crucial for understanding the depositional environment and potential subsurface applications.

Fourth, in this study, a limited set of subsurface metrics was used to compare and assess reservoir quality. Future work should include more metrics, like sand body connectivity and sand body volume, to help further understand the different behaviour of different modelling methods and combine it with subsurface research (Hariharan et al., 2021).

In summary, even limited by model simplifications and data availability, the research shows how the Reduced Complexity Model, namely DeltaRCM in this research, performs under similar parameters to a computationally demanding model (Delft3D) and its capacity to build geological models for real deltas, with focus on both surface and subsurface features. Addressing the limitations listed above can improve the reproductivity of DeltaRCM models and also contribute to future use of DeltaRCM in delta modelling.

6

Recommendations

This chapter builds on the issues and limitations mentioned in the previous chapters and proposes recommendations for further work in the field and on delta modelling.

6.1. Outcrop information

Before defining the reference model, the delta progradation direction and the direction and dimensions of the feeding channels should be reconciled with the field constraints (Joseph et al., 1993). Further study of paleochannels of the Roda Sandstone should quantify metrics including discharge, sinuosity, sediment concentration to provide target or validation datasets for future modelling (Sharma et al., 2023).

Bioturbation and carbonate are widespread in the Roda, yet their areal extent, thickness, and continuity remain uncertain. Mapping these features is essential for reservoir applications because they can influence flow paths.

Sea-level change, subsidence, and time in geological processes are not modelled in the same way as in nature, but they can provide insight into the source-to-sink condition. Porosity can be measured to indicate the extent of compaction due to diagenesis, offering insight into the geological processes that form the reservoir.

There's a lack of geophysical data at the scale needed for both model construction and validation. Geophysical exploration, such as GPR and ERT, has been conducted on the Roda Sandstone Z unit, helping to identify the distribution of primary heterogeneities (stratification) and the gradual compositional changes produced by diagenetic cementation (Coll et al., 2013). Such geophysical data can promote understanding of the internal heterogeneity within the Roda Sandstone and calibrate the geological model of the Roda.

6.2. DeltaRCM improvement

The priority is to improve the robustness of the DeltaRCM routing scheme, especially regarding the system's lateral water dispersion scheme. Enhancing the model stability will enable the model to remain stable across a range of hydrological conditions without failing. It might also improve the model performance in terms of backwater depth and overall water surface profile, which is essential for channel avulsion and lobe switching.

Adding carbonate sediments to the system is essential for subsurface applications for the Roda delta. Unlike siliclastic sand and mud in the existing DeltaRCM model, carbonate sediments (hardgrounds) are biogenic, thus a more scientifically accurate modelling approach would require the model to mimic the production, transport, and erosion of carbonate, and would require further understanding of both the palaeontology in the target formation (e.g., growth rate and population dynamics of shells in the

Roda) and the weighted random-walking algorithm of DeltaRCM. A recent study has developed a 3D forward stratigraphic model that simulates siliciclastic-carbonate mixed delta deposits in a tropical setting in Saudi Arabia (Baharudin et al., 2024), demonstrating the feasibility of adding carbonate features to the DeltaRCM system.

In the field, the Roda Sandstone (X and Y) has wave-induced deposits near the inlet channel and tidal sandstones near the seaward boundary (the Roda Y) (Crumeyrolle et al., 1992; A. W. Martinius, 2017). Adding a wave or tidal effect to the system is crucial for recreating the depositional environment. It is feasible to add the wave feature first by limiting the wave effect to reworking by applying this to wet cells within a certain distance of the shoreline. The wave effect should add weight to the neighbouring cells, biased on the along or onshore direction. Since DeltaRCM capacity is based on velocity, additional information is needed to determine whether wave reworking affects bedload and suspended load differently. To assess the tidal effect, coupling DeltaRCM models with external hydrodynamic forcings, such as tides, could also provide insight into the impact of tidal reworking in delta evolution (Bacopoulos et al., 2025).

The visualisation of delta evolution can also be improved by tracking key indicators of avulsion, such as the deceleration of lobe progradation and the increased mud concentration within the lobe (Xu et al., 2025). Monitoring this during runtime allows early identification of avulsion or bifurcation in the model.

7

Conclusion

This study constructed several geological models that mimic the development of Roda Sandstone X using DeltaRCM and evaluated its performance by comparing the results with the existing Delft3D model and the Roda field data. In this chapter, the findings are summarised by addressing the research questions and providing recommendations for future work.

7.1. Research questions

In the research, the following research questions need to be answered:

• Can we use a simpler and faster approach than Delft3D to generate a stratigraphic model similar to the Roda X?
Under the set-up of this research, we cannot use a simpler and faster approach than Delft3D to generate a stratigraphic model that is similar to the Roda X. The following three questions will explain it further.

- **What are the key input parameters needed for building the DeltaRCM model?**
  The main inputs controlling the DeltaRCM model include both domain parameters and hydraulic or sediment-related variables. These parameters include the grid and domain sizes, the subsidence rate, water discharge, sediment concentration, sand fraction, base level, slope, and the simulation duration (timesteps). In this research, sensitivity tests are conducted on discharge and sediment concentration, and water discharge has a greater influence on morphology and stratigraphic patterns. Higher discharge values promote stronger channel incision and lateral delta growth, while sediment concentration mainly affects the vertical accumulation rate.

- **Can DeltaRCM generate the lobe-like geometries at different scales, like those observed in the Roda Sandstone?**
  Under the settings used in this research, DeltaRCM does not reproduce lobe-like geometries at different scales comparable to those observed in the Roda Sandstone. Instead, DeltaRCM creates a single main lobe in the model that continues to prograde into the accommodation basin, with a strong channel-incised feature. However, in the field data, laterally and vertically stacked lobes with limited channel incisions are observed. Despite this limitation, DeltaRCM recreates delta-front deposits, a major facies in the Roda X, which form a large proportion of the geobody. This indicates that even though DeltaRCM generates delta models that have simplified large-scale geometry; it is still able to capture key depositional processes relevant to the Roda system.

- **What are the key similarities and differences between the stratigraphic architecture modelled by DeltaRCM and Delft3D, and the architecture deduced from field measurements?**
  Similarities:
  Both Delft3D and DeltaRCM generate delta models with similar dimensions and high sand fraction. Both models also reproduce major depositional elements, such as delta-front facies and delta lobes. However, neither modelling method can generate carbonate-cemented layers, which

are widely present in the model and have significant implications for reservoir applications.

Differences:
The Delft3D model generates a hierarchy of lobes and sublobes that better match observations in field data. By contrast, DeltaRCM creates a delta with one main lobe with strong channel incisions and lacks the lateral lobe switching and thus lacks a different hierarchy of lobes and sublobes. Field data from the Roda X shows multiple lobes and limited channel incision, which Delft3D better captures than DeltaRCM.

From this research, DeltaRCM provides a faster, more flexible approach to process-based delta modelling and sensitivity analysis. It effectively represents general depositional trends and large-scale stratigraphic architecture, such as the progradation of delta lobes and delta-front facies. Still, it does not create a delta model with multi-lobe evolution under the tested parameters, as seen in the Roda X. Even though Delft3D is more computationally demanding and time-consuming, it generates delta models that better capture the spatial complexity in the Roda X. Together, the research illustrates a trade-off between computational efficiency and geological accuracy between CFD models and RCM models.

7.2. Executive Summary

For further modelling in the Roda Sandstone
The Roda Sandstone generally shows intense wave- and tide-modified features. To better understand the spatial distribution of these geological features, additional fieldwork is needed, including facies mapping in plan view and through well logs, architecture and thickness statistics to capture tidal bundles and wave reworking, and paleocurrent studies to determine the direction of lobe progradation. Suppose further modelling of the Roda Sandstone explicitly aims to capture tidal and wave features. In that case, Delft3D is recommended over DeltaRCM, as the latter lacks wave or tidal modules in its algorithm and cannot reproduce tidal- and wave-induced flows.

For further delta modelling using DeltaRCM
Before using DeltaRCM to build geological models and perform sensitivity tests, it is vital to increase the model's robustness to address the issues identified in the previous chapter. For future applications, adding carbonate sedimentation/tidal and wave reworking enables the application of DeltaRCM to a broader range of geological settings beyond river-dominant deltas. It is also possible to add sediments of different grain sizes to the system to provide more realistic modelling results.

For industry
Under the current setting, Delft3D can create a delta model that resembles the outcrop of the Roda better than DeltaRCM. For further geological modelling in the delta area with coupled forcings, a hybrid workflow is recommended. Firstly, Delft3D should be used to generate realisations that incorporate tidal and wave dynamics and to extract the key metrics from the models. Then, DeltaRCM can be used to generate realisations in a relatively shorter time. By comparing the differences and similarities in the models, it promotes uncertainty qualification and guides static model construction and well placement.

Bibliography

Alghamdi, M. H. (2023). *Reservoir heterogeneity effect on co2 storage - investigate the effect of carbonate-cemented layers in the roda sandstone on the migration of the co2 plume at a short-term timescale using rrm and darts* [Master's thesis, Delft Univerisity of Technology].

Atlas, C. E. (2022). *New approaches to the architectural analysis of deltaic outcrops: Implications for subsurface reservoir characterization and analog selection* [Master's thesis, The University of Utah].

Bacopoulos, P., Ozdemir, C. E., & Hiatt, M. (2025). Rate of sea-level rise and sediment characteristics modulate deltaic river-tide interactions. *Water Resources Research*, *61*(8), e2024WR039056.

Baharudin, F., Herlambang, A., & Koeshidayatullah, A. (2024). 3d stratigraphic forward modeling of mixed carbonate-siliciclastic systems: Insights to energy prospectivity. *Geoenergy Science and Engineering*, *235*, 212699.

Bauer, S., Beyer, C., Dethlefsen, F., Dietrich, P., Duttmann, R., Ebert, M., Feeser, V., Görke, U., Köber, R., Kolditz, O., et al. (2013). Impacts of the use of the geological subsurface for energy storage: An investigation concept. *Environmental Earth Sciences*, 3935–3943.

Bhattacharya, J. P. (2006). Deltas. In H. W. Posamentier & R. G. Walker (Eds.), *Facies models revisited* (Vol. 84). SEPM Society for Sedimentary Geology.

Bokulich, A. (2013). Explanatory models versus predictive models: Reduced complexity modeling in geomorphology. In *Epsa11 perspectives and foundational problems in philosophy of science* (pp. 115–128). Springer.

Chan, N.-H., Langer, M., Juhls, B., Rettelbach, T., Overduin, P., Huppert, K., & Braun, J. (2023). An arctic delta reduced-complexity model and its reproduction of key geomorphological structures. *Earth Surface Dynamics*, *11*(2), 259–285.

Chanvry, E. (2016). *Caractérisation et facteurs de contrôle des distributions minéralogiques du bassin piggyback de graus-tremp-ainsa (espagne), à l'eocène inférieur.* [Doctoral dissertation, Université de Lyon].

Cohen, S., Jefferson, A. J., Czuba, J. A., Wohl, E., & McPhillips, L. E. (2022). Spatial trends and drivers of bedload and suspended sediment fluxes in global rivers. *Water Resources Research*, *58*(6), e2021WR031583. https://doi.org/10.1029/2021WR031583

Coll, M., López-Blanco, M., Queralt, P., Ledo, J., & Marcuello, A. (2013). Architectural characterization of a delta-front reservoir analogue combining ground penetrating radar and electrical resistivity tomography: Roda sandstone (lower eocene, graus–tremp basin, spain). *Geologica Acta*, *11*(1), 27–43. https://doi.org/10.1344/105.000001778

Crumeyrolle, P., Lesueur, J., Claude, D., & Joseph, P. (1992). Architecture et facies d'un prisme deltaique de bas niveau marin: Les gres de roda (basin eocene sud pyreneen). *Livret-guide de l'excursion ASF*, *25*.

Deltares. (2024). *New delft3d-geotool delta templates based on the roda and sobrarbe formations* [unpublished].

Durlofsky, L. J. (2005). Upscaling and gridding of fine scale geological models for flow simulation. *Proceedings of the 8th International Forum on Reservoir Simulation*.

Eichenseer, H., & Luterbacher, H. (1992). The marine paleogene of the tremp region (ne spain)-depositional sequences, facies history, biostratigraphy and controlling factors. *Facies*, *27*(1), 119–151.

Gearon, J. H., Martin, H. K., DeLisle, C., Barefoot, E. A., Mohrig, D., Paola, C., & Edmonds, D. A. (2024). Rules of river avulsion change downstream. *Nature*, *634*(8032), 91–95.

Geleynse, N., Storms, J. E., Walstra, D.-J. R., Jagers, H. A., Wang, Z. B., & Stive, M. J. (2011). Controls on river delta formation; insights from numerical modelling. *Earth and Planetary Science Letters*, *302*(1-2), 217–226.

Graham, G. H., Jackson, M. D., & Hampson, G. J. (2015). Three-dimensional modeling of clinoforms in shallow-marine reservoirs: Part 1. concepts and application. *AAPG Bulletin*, *99*(6), 1013–1047.

Hariharan, J., Xu, Z., Michael, H. A., Paola, C., Steel, E., & Passalacqua, P. (2021). Linking the surface and subsurface in river deltas—part 1: Relating surface and subsurface geometries. *Water Resources Research*, *57*(8), e2020WR029282.

Issautier, B., Viseur, S., Audigane, P., & Le Nindre, Y.-M. (2014). Impacts of fluvial reservoir heterogeneity on connectivity: Implications in estimating geological storage capacity for co_2. *International Journal of Greenhouse Gas Control*, *20*, 333–349. https://doi.org/10.1016/j.ijggc.2013.10.018

Joseph, P., Hu, L., Dubrule, O., & Claude, D. (1993). The roda deltaic complex (spain): From sedimentology to reservoir stochastic modelling. *COLLECTION COLLOQUES ET SEMINAIRES-INSTITUT FRANCAIS DU PETROLE*, *51*, 97–97.

Lauzon, R., Piliouras, A., & Rowland, J. C. (2019). Ice and permafrost effects on delta morphology and channel dynamics. *Geophysical Research Letters*, *46*(12), 6574–6582.

Leren, B. L., Howell, J., Enge, H., & Martinius, A. W. (2010). Controls on stratigraphic architecture in contemporaneous delta systems from the eocene roda sandstone, tremp-graus basin, northern spain. *Sedimentary Geology*, *229*(1-2), 9–40.

Lesser, G. R., Roelvink, J. v., van Kester, J. T. M., & Stelling, G. (2004). Development and validation of a three-dimensional morphological model. *Coastal engineering*, *51*(8-9), 883–915.

Liang, M., Voller, V., & Paola, C. (2015). A reduced-complexity model for river delta formation–part 1: Modeling deltas with channel dynamics. *Earth Surface Dynamics*, *3*(1), 67–86.

López-Blanco, M., Marzo, M., & Muñoz, J. A. (2003). Low-amplitude, synsedimentary folding of a deltaic complex: Roda sandstone (lower eocene), south-pyrenean foreland basin. *Basin Research*, *15*(1), 73–96.

Martinius, A. W. (2017). Multiscale gilbert-type delta lobe architecture and heterogeneities: The case of the roda sandstone member. *AAPG Bulletin*, *101*(4), 453–463.

Martinius, A., & Molenaar, N. (1991). A coral-mollusc (goniaraea-crassatella) dominated hardground community in a siliciclastic-carbonate sandstone (the lower eocene roda formation, southern pyrenees, spain). *PALAIOS 6.2*.

Meyer-Peter, E., & Müller, R. (1948). Formulas for bed-load transport. https://repository.tudelft.nl/record/uuid:4fda9b61-be28-4703-ab06-43cdc2a21bd7

Michael, H., Li, H., Boucher, A., Sun, T., Caers, J., & Gorelick, S. (2010). Combining geologic-process models and geostatistics for conditional simulation of 3-d subsurface heterogeneity. *Water Resources Research*, *46*(5).

Molenaar, N., & Martinius, A. (1990). Origin of nodules in mixed siliciclastic-carbonate sandstones, the lower eocene roda sandstone member, southern pyrenees, spain. *Sedimentary Geology*, *66*(3-4), 277–293.

Moodie, A. J., Hariharan, J., Barefoot, E., & Passalacqua, P. (2021). *pydeltarcm*: A flexible numerical delta model. *Journal of Open Source Software*, *6*(64), 3398. https://doi.org/10.21105/joss.03398

Moodie, A. J., Nittrouer, J. A., Ma, H., Carlson, B. N., Chadwick, A. J., Lamb, M. P., & Parker, G. (2019). Modeling deltaic lobe-building cycles and channel avulsions for the yellow river delta, china. *Journal of Geophysical Research: Earth Surface*, *124*(11), 2438–2462.

Moodie, A. J., & Passalacqua, P. (2021). When does faulting-induced subsidence drive distributary network reorganization? *Geophysical Research Letters*, *48*(22), e2021GL095053.

Muñoz, J. A. (1992). Evolution of a continental collision belt: Ecors-pyrenees crustal balanced cross-section. In *Thrust tectonics* (pp. 235–246). Springer.

Nichols, G. (2009). *Sedimentology and stratigraphy*. John Wiley & Sons.

Ojo, A. C., & Tse, A. C. (2016). Geological characterisation of depleted oil and gas reservoirs for carbon sequestration potentials in a field in the niger delta, nigeria. *Journal of Applied Sciences and Environmental Management*, *20*(1), 45–55.

Olariu, M. I., Olariu, C., Steel, R. J., Dalrymple, R. W., & Martinius, A. W. (2012). Anatomy of a laterally migrating tidal bar in front of a delta system: Esdolomada member, roda formation, tremp-graus basin, spain. *Sedimentology*, *59*(2), 356–378.

Ortiz-Sanguino, L., Vivas, C., Rehg, D., Knight, D., Perry, S., Bradley, A., Bedle, H., Salehi, S., & Marshall, S. (2022). Petrophysical modeling to improve the understanding of geothermal exploration in a sedimentary field on texas gulf coast basin. *Unconventional Resources Technology Conference, 20–22 June 2022*, 2446–2459.

Paola, C., & Mohrig, D. (1996). Palaeohydraulics revisited: Palaeoslope estimation in coarse-grained braided rivers. *Basin Research*, *8*, 243–254.

Puigdefabregas, C., Samsó, J., Serra-Kiel, J., & Tosquella, J. (1985). Facies analysis and faunal assemblages of the roda sandstone formation, eocene of the southern pyrenees. *International association of sedimentologists. European regional meeting. 6*, 639–642.

Puigdefàbregas, C., Muñoz, J., & Vergés, J. (1992). Thrusting and foreland basin evolution in the southern pyrenees. In *Thrust tectonics* (pp. 247–254). Springer.

Sandplover [Accessed: 2025-10-24]. (2021).

Sharma, N., Whittaker, A. C., Watkins, S. E., Valero, L., Vérité, J., Puigdefabregas, C., Adatte, T., Garcés, M., Guillocheau, F., & Castelltort, S. (2023). Water discharge variations control fluvial stratigraphic architecture in the middle eocene escanilla formation, spain. *Scientific Reports*, *13*(1), 6834.

Tinterri, R., et al. (2007). The lower eocene roda sandstone (south-central pyrenees): An example of a flood-dominated river-delta system in a tectonically controlled basin. *Rivista italiana di paleontologia e stratigrafia*, *113*(2), 223.

Wang, J., Dai, Z., Mei, X., Duan, H.-F., & Nienhuis, J. H. (2025). Response time of global deltas to changes in fluvial sediment supply. *Nature Communications*, *16*(1), 5573.

Wright, L. (1985). River deltas. In *Coastal sedimentary environments* (pp. 1–76). Springer.

Xu, Z.-H., Wu, S.-H., Liu, M.-C., Zhao, J.-S., Chen, Z.-H., Zhang, K., Zhang, J.-J., & Liu, Z. (2021). Effects of water discharge on river-dominated delta growth. *Petroleum Science*, *18*(6), 1630–1649.

Xu, Z.-H., Wu, S.-H., Plink-Björklund, P., Zhang, T., Yue, D.-L., Qian, Q.-H., Li, Q., & Feng, W.-J. (2025). Autocyclic switching processes and architecture of lobes in river-dominated lacustrine deltas. *Journal of Palaeogeography*, *14*(1), 126–140.